

## A General Approach to Co-operativity and its Application to the Oxygen Equilibrium of Hemoglobin and its Effectors

JUDITH HERZFELD† AND H. EUGENE STANLEY‡

††*Harvard-M.I.T. Program in Health Sciences and Technology*

†*Department of Chemistry, and ‡Department of Physics*

*Massachusetts Institute of Technology*

*Cambridge, Mass. 02139, U.S.A.*

*(Received 12 June 1972, and in revised form 14 May 1973)*

A general model of co-operativity is developed and solved explicitly; it combines the concepts of preferential binding and quaternary constraints (due to Monod, Wyman & Changeux), nearest-neighbor subunit interactions (due to Koshland), and changes in subunit aggregation (due to Briehl). For this reason, the general model can explain systems which previous models cannot—e.g. the model of Monod, Wyman & Changeux cannot explain negative co-operativity, the model of Koshland cannot treat situations where quaternary conformation is observed to be coupled to ligand binding, and the model of Briehl cannot explain co-operativity when no change in the level of subunit aggregation occurs. This general model of co-operativity reduces in special limits to these previous models. Still another limiting case corresponds to the Perutz description of hemoglobin, a “mixed” system thought to exhibit characteristics of several previous models.

Four distinct types of effector are defined and incorporated in the model. By calculating binding curves, and explicitly comparing them with experimental data concerning the inhibition of hemoglobin oxygenation by 2,3-diphosphoglycerate, one finds: (a) that  $P_2\text{Glyc}$  binding not only stabilizes the deoxy quaternary conformation of hemoglobin but also increases the strength of molecular (i.e. quaternary) constraints; (b) that the oxygen binding affinity is higher for the  $\alpha$  subunits than for the  $\beta$  subunits but that the  $\alpha$  and  $\beta$  subunits are practically equivalent with respect to the  $P_2\text{Glyc}$  binding equilibrium and molecular constraints; (c) that the quaternary conformation changes from the deoxy to the oxy form at about the third oxygenation, depending only slightly on  $P_2\text{Glyc}$  concentration; (d) that the detailed dependence of the four Adair parameters and of the apparent free energy of interaction on the free  $P_2\text{Glyc}$  concentration can be easily calculated; and (e) that the model describes biphasic oxygenation curves very well and can explain the dependence of the Hill coefficient,  $n_H$ , on  $P_2\text{Glyc}$  concentration, on pH, and on ionic strength.

The model is also used to describe the dependence of the oxygen equilibrium on hemoglobin concentration for very dilute solutions of HbA (normal adult hemoglobin) and for lamprey hemoglobin. It is found that oxygenated HbA dissociates more readily than deoxygenated HbA, primarily because the dimer has a very high oxygen affinity; the fact that the stability of the oxy quaternary conformation of the tetramer is somewhat lower than that of the deoxy quaternary conformation is relatively unimportant. For lamprey hemoglobin it is found that there is some tetramer present but one cannot tell whether the tetramer is co-operative like the HbA tetramer.

The model is finally applied to dimeric mollusc myoglobin, in order to try to determine the mechanism of co-operativity in this system from the temperature dependence of the oxygen equilibrium. This attempt proved unsuccessful in the temperature range of the data available.

† Present address: Department of Chemistry, Amherst College, Amherst, Mass 01002, U.S.A.

§ Abbreviations used:  $P_2\text{Glyc}$ , 2,3-diphosphoglycerate; MWC, Monod–Wyman–Changeux.

## 1. Introduction

When co-operativity was first discovered it was thought that the coupling of ligand binding at different sites on a protein molecule might be due to direct interactions between the bound ligands. However, it has since been found that the ligand binding sites are generally too distantly separated for direct interactions to account for the strength of the coupling observed. It is therefore necessary to hypothesize indirect interactions between sites in which the protein structure has an active role.

Several mechanisms have been proposed for such an indirect interaction. In all cases the protein molecule has two or more possible conformational states with different ligand binding affinities. By this process, called *preferential binding* (Monod *et al.*, 1965), the ligand binding equilibrium is coupled to the protein conformational equilibrium. An extreme case, in which the protein is exclusively in one conformational state when ligand is absent and in another conformational state when ligand is bound, is called *induced-fit binding* (Koshland *et al.*, 1966).

The various proposed mechanisms differ in the types of conformational change and the types of allosteric interactions attributed to the protein molecule. The conformational change(s) involved include: (i) a change in the state of aggregation of protein subunits (Briehl, 1963); (ii) a change in the quaternary conformation of a given aggregate of protein subunits (Monod *et al.*, 1965); and/or (iii) a change in the tertiary conformation of a specific protein subunit (Koshland *et al.*, 1966).

Proposed allosteric interactions may be: (i) between the quaternary equilibrium of the molecule and the tertiary equilibrium of each individual subunit (Monod *et al.*, 1965); or (ii) between the tertiary equilibria of neighboring subunits (Koshland *et al.*, 1966).

We shall refer to interactions of type (i) as *molecular constraints*, or quaternary-tertiary (q-t) interactions. Type (ii) interactions will be called *nearest-neighbor constraints*, or tertiary-tertiary (t-t) interactions. For either type, the extreme of infinitely strong constraints corresponds to concerted change of all subunit conformations.

Both types of allosteric interactions, (i) and (ii), have their strengths and their weaknesses. Molecular constraints can describe positive but not negative co-operativity. Ligand binding stabilizes the quaternary state with the higher ligand affinity and thereby facilitates further ligand binding. Nearest-neighbor constraints, however, can explain both positive and negative co-operativity. If a pair of neighboring subunits are more stable when they are in the same conformation, then positive co-operativity will occur; if they are more stable when in unlike conformations, negative co-operativity may occur. On the other hand, nearest-neighbor constraints cannot explain situations where the state of aggregation and the quaternary structure are observed to depend on ligand binding. This coupling can be explained by molecular constraints.

The indirect coupling of ligand binding at different sites, due to the combination described above of preferential binding, conformational change, and allosteric interactions, is illustrated schematically in Figure 1.

In the work described here, we have combined all the above concepts, *generalized* from earlier models, into a single quantitative model which is applicable to a wide variety of systems. We illustrate our approach by considering the oxygenation of hemoglobin in some detail. Perutz (1970*a,b*) has proposed that the behavior of

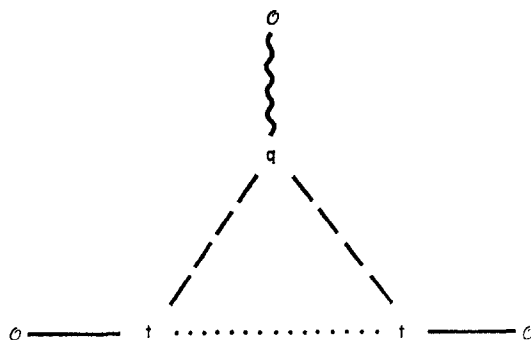


FIG. 1. Schematic representation of the indirect coupling of ligand binding at different sites. The symbols  $q$  and  $t$  represent the quaternary conformation of the molecule and the tertiary conformation of a subunit, respectively, while  $\emptyset$  represents the occupancy (i.e. occupied or vacant) of a ligand binding site. The notations (-----) and (.....) represent molecular constraints ( $q$ - $t$  interactions) and nearest-neighbor constraints ( $t$ - $t$  interactions), respectively, while (——) and (~~~~) represent preferential ligand binding to different tertiary and quaternary conformations, respectively.

HbA (normal adult hemoglobin) combines aspects of both the MWC<sup>†</sup> and Koshland theories. The co-operative mechanism is thought to consist of molecular constraints, as suggested by MWC, and induced-fit binding, as suggested by Koshland. Our model provides a quantitative test of this hybrid picture against oxygenation data. We shall see that the picture becomes still more complex at very low hemoglobin concentrations, where the effect of ligand-dependent disaggregation of the tetramer must be taken into account. In addition, we consider the action of effectors of oxygenation, in particular the inhibitor 2,3-diphosphoglycerate.

## 2. The Model

Following Monod *et al.* (1965) and Koshland *et al.* (1966), we suppose that the states of the protein molecule may be adequately described by the following gross features:

- (1) the association of ligands with binding sites,
- (2) the tertiary conformations of each of the subunits,
- (3) the quaternary arrangement of the subunits, and
- (4) the total number,  $N$ , of equivalent subunits in the molecule.

All combinations of occupancy of sites, tertiary conformations of subunits, quaternary conformation, and level of subunit aggregation can *conceivably* exist, but some of these states may be much less probable than others. We assume the following constraints exist (see discussion in the Introduction above): (1) preferential ligand binding, (2) nearest-neighbor constraints, and (3) molecular constraints.

We shall assume that the ligand of primary interest, called the substrate, has one or more binding sites on each subunit, and can therefore exhibit homotropic co-operativity. Other ligands, called effectors, may affect substrate binding in the four mutually *non-exclusive* ways illustrated in Figure 2.

<sup>†</sup> See footnote § to p. 231 for abbreviations used.

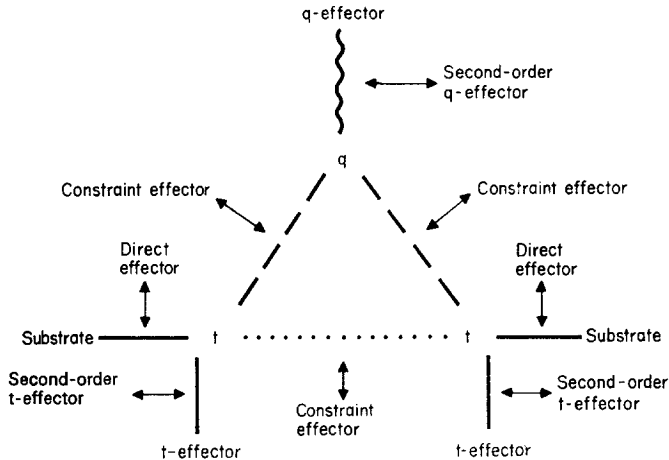


FIG. 2. A schematic representation of different types of effector action. The symbol  $\leftrightarrow$  represents effector binding which changes the strength of the allosteric and/or preferential binding interactions that are represented by the symbols used in Fig. 1.

(1) *Allosteric effectors* are molecules that shift the equilibrium between accessible conformations by binding preferentially to a particular tertiary or quaternary conformation; these we call tertiary and quaternary effectors, respectively (or, for short, *t-effectors* and *q-effectors*). Since salt bridges are broken when subunits change from the deoxy to the oxy tertiary conformation (Perutz, 1970*a,b*), and since hydrogen ions bind preferentially to the intact salt bridges, hydrogen ions are *t-effectors* of hemoglobin oxygenation. Similarly, since  $P_2$ Glyc binds preferentially to the deoxy quaternary conformation of hemoglobin (Perutz, 1970*a,b*),  $P_2$ Glyc is a *q-effector*. Note that by so altering the equilibrium between quaternary conformations, *q-effectors* may help us to understand the role which changes in quaternary structure have in the co-operative mechanism.

(2) *Direct effectors* are molecules that interact directly with bound substrate molecules, or with the substrate receptors, thereby changing the stability of the bound complex and the observed binding affinity. In the limiting case of extreme antagonistic interactions between substrate and effector, binding of two ligands is mutually exclusive. For this case, effector binding competes with substrate binding and the effector is called a *competitive effector*. (Although they may be physically competing for occupancy of the same binding sites, it is conceptually convenient to think in terms of an interaction between two distinct binding events.) Carbon monoxide is an example of a competitive effector of hemoglobin oxygenation.

(3) *Constraint effectors* are molecules that bind to the protein molecule in such a way as to alter the strength of the *t-t* interactions or the *q-t* interactions. As we shall see in section 5 below,  $P_2$ Glyc acts, in part, as a constraint effector of hemoglobin oxygenation, strengthening the *q-t* interactions.

(4) *Second-order effectors* shift the equilibrium between accessible conformations *indirectly*, by interacting with bound effectors, or with their receptors. This alters the binding affinities of the effectors and therefore their effect on substrate binding.

Since hydrogen ions affect P<sub>2</sub>Glyc binding to hemoglobin (Benesch *et al.*, 1969), hydrogen ions are second-order quaternary effectors of hemoglobin oxygenation, as well as t-effectors (as described above).

In this paper we make the assumption that each subunit interacts with exactly two neighboring subunits (the "square model"). An alternative assumption, that each subunit interacts equivalently with all other subunits (the "tetrahedral model"), is not discussed here (although the mathematics involved is simpler than for the square model) because it is less relevant for our applications to hemoglobin.

Our goal is to calculate the substrate binding curves for the above model. The fraction of substrate binding sites occupied by substrate,  $Y_s$ , is given by the simple expression

$$Y_s = \frac{\sum n f}{\sum N f} \quad (1)$$

Here the summations are over all possible states of the protein molecule (see the first paragraph of this section).  $n = n(\text{state})$  is the number of substrate sites occupied in that state,  $N = N(\text{state})$  is the total number of substrate sites available in that state (one site per subunit) and  $f = f(\text{state})$  is the fraction of molecules which is in a given state.

According to the standard statistical assumption, the fraction  $f$  of a large number of molecules which is in a given state is equal to the probability  $P$  that a single molecule will be in that state. Thus in the absence of effector binding,

$$f = P = \frac{\exp(n\mu_s/kT) \exp(N\mu_p/kT) \exp(-E/kT)}{Z} = \frac{\exp(-\mathcal{E}/kT)}{Z}, \quad (2)$$

where  $\mu_s$  is the chemical potential of substrate,  $\mu_p$  is the chemical potential of unliganded subunits,  $E = E(\text{state})$  is the energy of a given state,  $\mathcal{E} \equiv -n\mu_s - N\mu_p + E$ , and  $Z$  is the normalization constant, determined by the condition that the sum of probabilities of all states add to unity,

$$Z = \sum_{\text{all states}} \exp(n\mu_s/kT) \exp(N\mu_p/kT) \exp(-E/kT) = \sum_{\text{all states}} \exp(-\mathcal{E}/kT). \quad (3)$$

(The symbol  $Z$  is used because  $Z$  is the partition function of statistical mechanics; see, for example, Davidson (1962).  $Z$  is related to the binding potential,  $\Pi$ , introduced by Wyman (1965,1967,1968) by the equation  $Z = \exp(\Pi/RT)$ .) Combining eqns (1) and (3), we can express the fraction of occupied substrate sites directly in terms of  $Z$ ,

$$Y_s = \left( \frac{\partial Z}{\partial \mu_s/kT} \right) / \left( \frac{\partial Z}{\partial \mu_p/kT} \right). \quad (4)$$

Notice that if the zero of energy is shifted by a constant (i.e.  $Z$  is multiplied by a constant) eqn (4) remains valid.

### 3. Substrate Binding Curves

To obtain  $Y_s$ , as shown in section 2 above, it suffices to calculate  $Z$ , where  $Z$  is a function of the energies of the possible states of the protein molecule. In order to calculate  $Z$ , it is first necessary to specify the states of the protein molecule. These can be represented by a set of *state variables*, each describing an important feature of the molecule.

- (1) The occupancy of the substrate site on  $i$ th subunit is given by  $\mathcal{O}_i$ , where  $\mathcal{O}_i$  takes on the values 0, 1 according to whether the site is vacant or occupied.
- (2) The tertiary conformation of the  $i$ th subunit is given by  $t_i$ , where  $t_i = k$  indicates that the  $i$ th subunit is in the tertiary conformation  $k$  ( $k = 1, 2, \dots$ ).
- (3) The quaternary conformation is given by  $q$ , where  $q = k$  indicates that the protein molecule is in the quaternary conformation  $k$  ( $k = 1, 2, \dots$ ).
- (4) The level of aggregation is specified by  $N$ , the total number of subunits.

Using this notation, eqn (3) can be rewritten in the form

$$Z = \sum_{\mathcal{O}_1} \dots \sum_{\mathcal{O}_N} \sum_{t_1} \dots \sum_{t_N} \sum_q \exp(-\mathcal{E}/kT), \quad (5a)$$

or in the abbreviated form

$$Z = \sum_{\{\mathcal{O}_i\}} \sum_{\{t_i\}} \sum_q \exp(-\mathcal{E}/kT). \quad (5b)$$

$Z$  is calculated explicitly for the general case in the Appendix. However, for hemoglobin tetramer ( $N = 4$ ), it suffices to assume that there are only two possible quaternary conformations for the molecule (the deoxy and oxy conformations, corresponding to  $q = 1$  and 2, respectively) and only two possible tertiary conformations for each subunit (the deoxy and oxy conformations of the subunit, corresponding to  $t_i = 1$  and  $t_i = 2$ , respectively). Then for a particular state of the molecule, the quantity  $\mathcal{E}$  that appears in eqn (3) is given by the expression

$$\mathcal{E} = U_q q + \sum_{i=1}^4 \{U t_i + [-\mu_{\text{O}_2} + U_\theta + (-1)^{t_i} U_{\theta t}] \mathcal{O}_i - U_{tt}(q)(-1)^{t_i+t_{i+1}} - U_{qt}(-1)^{t_i+q}\}, \quad (6)$$

where  $U_q$  is the difference in energy between the two quaternary conformations of the molecule,  $U_t$  is the difference in energy between the two tertiary conformations of a given subunit,  $U_\theta + (-1)^{t_i} U_{\theta t}$  is the energy of substrate binding to a subunit in the  $t_i$  tertiary conformation,  $-U_{tt}(-1)^{t_i+t_{i+1}}$  is the energy of interaction between neighboring subunits in the tertiary conformations  $t_i$  and  $t_{i+1}$ , and  $-U_{qt}(-1)^{t_i+q}$  is the energy of the constraint on a subunit in the  $t_i$  tertiary conformation when the molecule is in the  $q$  quaternary conformation. (Note that the zero of energy has been shifted by the amount  $-4\mu_p$ .)

Combining eqns (5) and (6) results in the expression

$$Z = \sum_q \exp(-U_q q/kT) \sum_{\{t_i\}} \prod_{i=1}^4 \exp(-[U t_i - U_{tt}(q)(-1)^{t_i+t_{i+1}} - U_{qt}(-1)^{t_i+q}]/kT) \times \{1 + \exp(-[-\mu_{\text{O}_2} + U_\theta + (-1)^{t_i} U_{\theta t}]/kT)\}. \quad (7)$$

Applying the methods of the Appendix, we arrive at the result

$$Z = \{[\chi_+(1)]^4 + [\chi_-(1)]^4\} + \exp(-U_q/kT) \{[\chi_+(2)]^4 + [\chi_-(2)]^4\}, \quad (8)$$

where

$$\chi_{\pm}(q) = \exp(U_{tt}(q)/kT) \{\phi(1|q) + \phi(2|q)\} / 2 \pm [\exp(2U_{tt}(q)/kT) \{\phi(1|q) - \phi(2|q)\}^2 / 4 + \exp(-2U_{tt}(q)/kT) \{\phi(1|q)\phi(2|q)\}]^{1/2}. \quad (9)$$

The quantities  $\phi(t|q)$  appearing in eqn (9) are defined through the relations (cf. Appendix),

$$\phi(1|q) \equiv (1 + K_1 p_{O_2}) \exp[-(-1)^q U_{qt}/kT] \quad (10a)$$

and

$$\phi(2|q) \equiv \exp(-U_t/kT)(1 + K_2 p_{O_2}) \exp((-1)^q U_{qt}/kT). \quad (10b)$$

$K_1$  and  $K_2$  are the binding constants for oxygen binding to subunits in the deoxy and oxy tertiary conformations respectively,

$$p_{O_2} K_1 = \exp(\mu_{O_2}/kT) \exp(-[U_\sigma - U_{\sigma t}]/kT) \quad (11a)$$

and

$$p_{O_2} K_2 = \exp(\mu_{O_2}/kT) \exp(-[U_\sigma + U_{\sigma t}]/kT). \quad (11b)$$

The fraction of oxygenated sites is then given directly in terms of  $Z$  by means of eqn (4), which becomes

$$Y_{O_2} = \frac{\partial Z}{\partial(\mu_{O_2}/kT)} / (4Z) = (1/4) \frac{\partial \ln Z}{\partial \ln p_{O_2}}. \quad (12)$$

The behavior of a protein molecule is specified by the values of the parameters  $U_\sigma$ ,  $U_{\sigma t}$ ,  $U_q$ ,  $U_{tt}(q)$  and  $U_{qt}$  for the particular system. Some special cases are the following:

(A) If  $U_{tt}(q) \cong 0$  (i.e.  $U_{tt}(q) \ll kT$  so  $\exp[U_{tt}(q)/kT] \cong 1$ ), then we can neglect nearest-neighbor constraints and co-operativity is entirely due to molecular constraints.

(B) If  $U_{qt} \cong 0$  (i.e.  $U_{qt} \ll kT$ ), then we can neglect molecular constraints and co-operativity is entirely due to nearest-neighbor constraints.

(C) If  $U_{\sigma t} \cong 0$  (i.e.  $U_{\sigma t} \ll kT$ ) the substrate binding affinity is essentially independent of the tertiary structure of the subunit (i.e. substrate binding is not preferential) and substrate binding to sites on different subunits is always independent.

(D) If  $U_{qt} \rightarrow \infty$  (i.e.  $U_{qt} \gg kT$  so  $\exp(-U_{qt}/kT) \cong 0$ ), then  $t_i = q$ , for all  $i$ , because all other conformational states have infinite interaction energies and therefore have zero probability. Thus when  $U_{qt} \rightarrow \infty$ , the molecule undergoes a concerted change of tertiary and quaternary conformation; there are no hybrid states.  $U_{qt} \rightarrow \infty$  is known as the "symmetry" assumption (Monod *et al.*, 1965).

(E) If  $U_{tt}(q) \rightarrow \infty$  (i.e.  $U_{tt}(q) \gg kT$ ) then, when the oligomer is in the  $q$  quaternary conformation,  $t_i = t_j$  for all  $i, j$ , because any pair of nearest-neighbor subunits in unlike conformations has an infinite interaction energy and, therefore, zero probability. Thus, when  $U_{tt}(q) \rightarrow \infty$ , there is a *concerted change* of all tertiary conformations within the  $q$ -quaternary structure. Thus,  $U_{tt}(q) \rightarrow \infty$  is similar, but not identical, to the symmetry assumption ( $U_{qt} \rightarrow \infty$ ).

(F) If  $U_t \rightarrow \eta \infty$  and  $U_{\sigma t} \rightarrow -\eta \infty$  with  $\eta = \pm 1$  (i.e.  $|U_{\sigma t}| \gg kT$  and  $|U_t| \gg kT$ , but  $(U_{\sigma t} + U_t)$  is finite), then  $t_j = (3 - \eta)/2$  in the absence of substrate and  $t_j = (3 + \eta)/2$  when substrate is bound because all other states have infinitely greater energy and zero probability. Thus, substrate binding determines, or induces, the tertiary conformation. This is known as the "induced-fit" assumption (Koshland *et al.*, 1966).

We next show how the models of hemoglobin oxygenation proposed by Monod *et al.* (1965), Koshland *et al.* (1966), and Perutz (1970*a,b*) correspond to particular cases of the general model described in this work. In the MWC model, it is assumed that there are no nearest-neighbor constraints (case A above) but that molecular constraints are infinite (case D). The reader will note that eqns (8) to (12) give the MWC equations for the oxygen equilibrium of hemoglobin when  $U_{it}(q) \rightarrow 0$  and  $U_{qt} \rightarrow \infty$ .

The Koshland model assumes that there are no molecular constraints (case B) and that induced-fit binding occurs (case F). Thus eqns (8) to (12) give the Koshland—and, equivalently, the Pauling (1935) and Thompson (1968)—equations for hemoglobin oxygenation when  $U_{qt} \rightarrow 0$ ,  $U_t \rightarrow \infty$ , and  $U_{\theta t} \rightarrow -\infty$  (with  $U_{\theta t} + U_t$  finite).

Perutz has recently suggested that for HbA there are no nearest-neighbor constraints, as in the MWC model, but that molecular constraints are finite, unlike the MWC model. Perutz has also suggested that oxygen binding is induced fit. Thus, the Perutz picture corresponds to the limit  $U_{it} \rightarrow 0$ ,  $U_t \rightarrow \infty$ , and  $U_{\theta t} \rightarrow -\infty$  (with  $U_{\theta t} + U_t$  finite), and eqns (8) to (10) reduce to

$$Z = (1 + K_{\text{deoxy}}p_{\text{O}_2})^4 + \exp(-U_q^*/kT)(1 + K_{\text{oxy}}p_{\text{O}_2})^4, \quad (13a)$$

where  $U_q^*$  is the difference in the total conformational energy (quaternary energy and constraint energy) between the deoxy and oxy quaternary conformations of the molecule in the absence of oxygen

$$U_q^* = U_q + 8U_{qt}. \quad (13b)$$

According to eqn (12),

$$Y_{\text{O}_2} = \left[ \frac{K_{\text{deoxy}}(1 + K_{\text{deoxy}}p_{\text{O}_2})^3 + \exp(-U_q^*/kT)K_{\text{oxy}}(1 + K_{\text{oxy}}p_{\text{O}_2})^3}{(1 + K_{\text{deoxy}}p_{\text{O}_2})^4 + \exp(-U_q^*/kT)(1 + K_{\text{oxy}}p_{\text{O}_2})^4} \right] p_{\text{O}_2}. \quad (14)$$

Here  $K_{\text{deoxy}}$  and  $K_{\text{oxy}}$  are the binding constants for *induced-fit* oxygen binding to subunits *constrained* by the deoxy and oxy quaternary conformations respectively, and are given by

$$K_{\text{deoxy}} = \exp(-2U_{qt}/kT)K \quad (15a)$$

and

$$K_{\text{oxy}} = \exp(2U_{qt}/kT)K, \quad (15b)$$

where  $K$  is the binding constant for *induced-fit* oxygen binding to a subunit in the *absence* of molecular constraints,

$$p_{\text{O}_2}K = \exp(\mu_{\text{O}_2}/kT) \exp(-(U_{\theta} + U_{\theta t} + U_t)/kT). \quad (15c)$$

(The reader should note the distinction between these induced-fit binding constants and the binding constants  $K_1$  and  $K_2$  defined in eqn (11).)

It is significant that eqn (14) is of the same form as the oxygenation equation arising from the MWC model. This is to be expected, since the MWC and Perutz pictures are equivalent with respect to oxygenation—i.e. substrate binding at different sites is interrelated in the same way in the two models. This fact may be verified by examining the relationships between the boxes in the diagram of Figure 3. The only difference between the MWC and Perutz models is that for the MWC model the tertiary conformation is determined by the quaternary conformation (due to the symmetry assumption) and for the Perutz model the tertiary conformation is determined by substrate binding (due to the induced-fit binding assumption). Thus

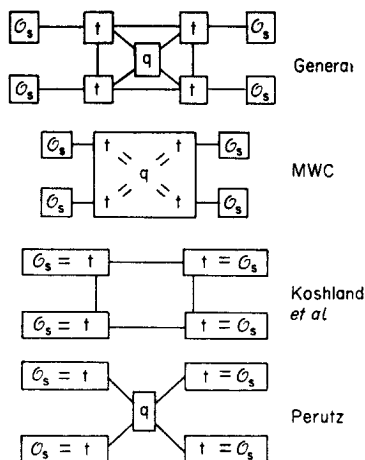


FIG. 3. Various allosteric mechanisms for homotropic co-operativity in a tetramer are shown as special cases of the general model. The notation  $O_s$ ,  $t$ ,  $q$  corresponds respectively to substrate binding, tertiary conformation, and quaternary conformation. A solid line indicates an interaction, while a double line, together with an enclosing box, indicates an infinitely strong interaction.

the two models give the same oxygenation equations, although the parameters of the equations have different microscopic meanings for each model. Thus, if these parameters are regarded as “adjustable parameters” to be determined by a best fit to the observed data, then the two models should be capable of describing data with equal “accuracy”. This explains why the MWC model provides a good fit to data (Monod *et al.*, 1965; Ogata & McConnell, 1972a) even if the underlying mechanism of co-operativity in hemoglobin is better described by the microscopic details afforded by the Perutz picture.

#### 4. Effector Action

The expressions developed in the previous section describe hemoglobin oxygenation in the absence of effectors. In order to describe effector action, it is necessary to modify eqns (5) and (6).

Consider first the case in which there is one effector binding site on each subunit. Let the *effector* chemical potential be represented by  $\mu_e$  and let the state variable  $\bar{\theta}_i$  represent the occupancy of the *effector* binding site on the  $i$ th subunit (where  $i = 1, 2, \dots, N$ ). Then the sum over states in eqn (5) must be expanded to include all possible effector binding states,

$$Z = \sum_{\bar{\theta}_1} \dots \sum_{\bar{\theta}_N} \sum_{\theta_1} \dots \sum_{\theta_N} \sum_{t_1} \dots \sum_{t_N} \sum_q \exp(-\mathcal{E}/kT) \quad (16a)$$

$$= \sum_{\{\bar{\theta}_i\}} \sum_{\{\theta_i\}} \sum_{\{t_i\}} \sum_q \exp(-\mathcal{E}/kT). \quad (16b)$$

The energy  $\mathcal{E}$ , given in eqn (6), must be modified to include the additional energy,  $\delta\mathcal{E}$ , associated with effector binding. For a tertiary effector, the energy term that must be added to  $\mathcal{E}$  is of the form

$$\delta \mathcal{E} = \sum_{i=1}^N [-\mu_o + U_{\bar{o}} + (-1)^i U_{\bar{o}i}] \bar{\theta}_i. \quad (17)$$

Combining eqns (16), (6), and (17), we obtain the partition function for the case in which there exists a tertiary effector,

$$\begin{aligned} Z = \sum_q \exp(-U_{qg}/kT) \sum_{\{t_i\}} \prod_{i=1}^N \exp(-[U_{it_i} - U_{it_i}(q)(-1)^{t_i+t_i+1} - U_{qt}(-1)^{t_i+q}]/kT) \\ \times \{1 + \exp(-[-\mu_s + U_{\bar{o}} + (-1)^{t_i} U_{\bar{o}t_i}]/kT)\} \\ \times \{1 + \exp(-[-\mu_o + U_{\bar{o}} + (-1)^{t_i} U_{\bar{o}t_i}]/kT)\}. \end{aligned} \quad (18)$$

Eqn (18) can be rewritten in the form of eqn (7),

$$\begin{aligned} Z = \sum_q \exp(-U_{qg}/kT) \sum_{\{t_i\}} \prod_{i=1}^N \\ \exp(-[\hat{U}_{it_i} - U_{it_i}(q)(-1)^{t_i+t_i+1} - U_{qt}(-1)^{t_i+q}]/kT) \\ \times \{1 + \exp(-[-\mu_s + U_{\bar{o}} + (-1)^{t_i} U_{\bar{o}t_i}]/kT)\}, \end{aligned} \quad (19)$$

where

$$\exp(-\hat{U}_{it_i}/kT) \equiv \left( \frac{1 + \exp(-[-\mu_o + U_{\bar{o}} + U_{\bar{o}t_i}]/kT)}{1 + \exp(-[-\mu_o + U_{\bar{o}} - U_{\bar{o}t_i}]/kT)} \right) \exp(-U_{it_i}/kT). \quad (20)$$

The influence of a tertiary effector is summarized by eqn (20), which shows the complex dependence of the *effective* tertiary conformational energy,  $\hat{U}_t$ , on effector chemical potential and temperature. Since  $\hat{U}_t$  is constant if the chemical potential of the effector *and* the temperature are held constant during oxygenation, the equations of section 3 above—developed for oxygenation in the absence of effector—can describe oxygenation in the presence of tertiary effector at a single chemical potential and at a single temperature.

Notice in eqn (20) that at very high effector concentrations,

$$\hat{U}_t \cong U_t + 2U_{\bar{o}t}, \quad (21a)$$

and that at very low effector concentrations,

$$\hat{U}_t \cong U_t. \quad (21b)$$

If  $U_{\bar{o}t}$  is very large, then at intermediate effector concentrations,

$$\hat{U}_t \cong U_t - [-\mu_o + U_{\bar{o}} - U_{\bar{o}t}], \quad (21c)$$

and if  $-U_{\bar{o}t}$  is very large, then at intermediate effector concentrations,

$$\hat{U}_t \cong U_t + [-\mu_o + U_{\bar{o}} + U_{\bar{o}t}]. \quad (21d)$$

Thus at *certain* levels of effector concentration, the temperature dependence of  $\hat{U}_t$  may be neglected, and, for a constant effector concentration at any of these levels, the equations of section 3—developed for oxygenation in the absence of effector—can describe the *temperature dependence* of oxygenation in the presence of tertiary effector.

A similar analysis may be performed for the case of a direct effector. In this case

$$\delta \mathcal{E} = \sum_{i=1}^N [-\mu_o + U_{\bar{o}} + \theta_i U_{\bar{o}\bar{o}}] \bar{\theta}_i. \quad (22)$$

The partition function  $Z$  may be written in the form of eqn (7), with  $U_{\theta}$  replaced by  $\hat{U}_{\theta}$ , where

$$\exp(-\hat{U}_{\theta}/kT) \equiv \exp(-U_{\theta}/kT) \left( \frac{1 + \exp(-[-\mu_o + U_{\bar{o}} + U_{\bar{o}\bar{o}}]/kT)}{1 + \exp(-[-\mu_o + U_{\bar{o}}]/kT)} \right). \quad (23)$$

Since  $\hat{U}_{\theta}$  is constant if the effector chemical potential *and* the temperature are held constant, the equations of section 3 can describe oxygenation at a single effector chemical potential and at a single temperature. Since  $\hat{U}_{\theta}$  is nearly independent of temperature in certain ranges of  $\mu_o$ , the equations of section 3 can describe the temperature dependence of oxygenation at a single effector chemical potential in any of these ranges.

For a constraint effector,

$$\delta \mathcal{E} = [-\mu_o + U_{\bar{o}} - (-1)^{q+t_i} U_{\bar{o}q t_i}] \bar{\theta}_i \quad (24a)$$

when q-t interactions are changed by the effector (cf. Fig. 2), or

$$\delta \mathcal{E} = [-\mu_o + U_{\bar{o}} - (-1)^{t_i+t_i+1} U_{\bar{o} t_i}] \bar{\theta}_i \quad (24b)$$

when t-t interactions are involved. When  $Z$  is written in the form of eqn (7),  $U_{qt}$  (or  $U_{tt}$ ) is replaced by  $\hat{U}_{qt}$  (or  $\hat{U}_{tt}$ ), where

$$\exp(2\hat{U}_{qt}/kT) \equiv \exp(2U_{qt}/kT) \left( \frac{1 + \exp(-[-\mu_o + U_{\bar{o}} - U_{\bar{o}q t}]/kT)}{1 + \exp(-[-\mu_o + U_{\bar{o}} + \hat{U}_{\bar{o}q t}]/kT)} \right), \quad (25a)$$

and

$$\exp(2\hat{U}_{tt}/kT) \equiv \exp(2U_{tt}/kT) \left( \frac{1 + \exp(-[-\mu_o + U_{\bar{o}} - U_{\bar{o} t t}]/kT)}{1 + \exp(-[-\mu_o + U_{\bar{o}} + U_{\bar{o} t t}]/kT)} \right). \quad (25b)$$

As before, the equations of section 3 can describe oxygenation at constant temperature and constant effector chemical potential. At certain chemical potentials the equations of section 3 can also describe the temperature dependence of oxygenation.

Some effectors, such as quaternary effectors, do not bind to each subunit but rather bind to a single site on the molecule. For a quaternary effector,

$$\delta \mathcal{E} = [-\mu_o + U_{\bar{o}} + (-1)^q U_{\bar{o}q}] \bar{\theta}, \quad (26)$$

where  $\bar{\theta} = 0, 1$  according as this single site is empty or occupied. When  $Z$  is written in the form of eqn (7),  $U_q$  is replaced by  $\hat{U}_q$ , where

$$\exp(-\hat{U}_q/kT) \equiv \exp(-U_q/kT) \left( \frac{1 + \exp(-[-\mu_o + U_{\bar{o}} + U_{\bar{o}q}]/kT)}{1 + \exp(-[-\mu_o + U_{\bar{o}} - U_{\bar{o}q}]/kT)} \right). \quad (27)$$

Once again the equations of section 3 are adequate to describe oxygenation at constant temperature and effector chemical potential; at certain effector chemical potentials, they can also describe the temperature dependence of oxygenation.

A single effector, such as  $H^+$ , may bind at many different types of sites. So long as the effector action at *each* site is of only one type (e.g. direct effector, constraint effector, . . .), then the above analysis and conclusions still hold. However, if binding of effector at one site has more than one type of effect, the above analysis does not carry through—i.e. the equations of section 3 cannot describe oxygenation completely accurately, even at constant temperature and constant effector chemical potential. In the following section we shall see that  $P_2\text{Glyc}$  is such an effector.

## 5. 2,3-Diphosphoglycerate

### (a) 2,3-Diphosphoglycerate as a quaternary effector

As noted in section 2 above, since  $P_2\text{Glyc}$  binds preferentially to the deoxy quaternary conformation of hemoglobin, it is by definition a quaternary effector.

We have shown in section 4 that the equations of section 3 can describe hemoglobin oxygenation at a constant concentration of quaternary effector and a constant temperature. However, we would like to understand the changes in hemoglobin oxygenation when the concentration of  $P_2\text{Glyc}$  is varied.

In order to calculate  $Y$  in the presence of  $P_2\text{Glyc}$ , we add the energy  $\delta\mathcal{E} = [-\mu_{P_2\text{Glyc}} + U_\delta + (-1)^q U_{\delta q}] \bar{\mathcal{G}}$  of eqn (26) to the energy  $\mathcal{E}$  given by eqn (6). Then by exactly the same methods that led to eqn (13), we obtain the appropriate generalization to arbitrary  $P_2\text{Glyc}$  concentration of the partition function,

$$Z = (1 + \tilde{K}_{\text{deoxy}} [P_2\text{Glyc}]_{\text{free}}) (1 + K_{\text{deoxy}} p_{O_2})^4 + (1 + \tilde{K}_{\text{oxy}} [P_2\text{Glyc}]_{\text{free}}) \exp(-U_q^*/kT) (1 + K_{\text{oxy}} p_{O_2})^4. \quad (28)$$

Here  $[P_2\text{Glyc}]_{\text{free}}$  denotes the concentration of free  $P_2\text{Glyc}$ ;  $\tilde{K}_{\text{deoxy}}$  and  $\tilde{K}_{\text{oxy}}$ , the binding constants for  $P_2\text{Glyc}$  binding to the deoxy and oxy quaternary conformations, respectively, are defined through the relations

$$[P_2\text{Glyc}]_{\text{free}} \tilde{K}_{\text{deoxy}} = \exp(\mu_{P_2\text{Glyc}}/kT) \exp(-(U_\delta - U_{\delta q})/kT) \quad (29a)$$

$$[P_2\text{Glyc}]_{\text{free}} \tilde{K}_{\text{oxy}} = \exp(\mu_{P_2\text{Glyc}}/kT) \exp(-(U_\delta + U_{\delta q})/kT). \quad (29b)$$

In eqns (15), (28) and (29), all the energies are dependent upon the chemical potential of effectors *other* than  $P_2\text{Glyc}$  and perhaps on temperature (cf. discussion in section 4).

From the expression of eqn (28) for the partition function  $Z$  we can calculate, using eqn (4), the fraction of heme groups that are oxygenated,

$$Y_{O_2} = \frac{1}{4} \frac{\partial \ln Z}{\partial \ln p_{O_2}} \quad (30)$$

Similarly, we can calculate from  $Z$  the fraction of hemoglobin molecules with  $P_2\text{Glyc}$  bound,

$$\tilde{Y}_{P_2\text{Glyc}} = \frac{\partial \ln Z}{\partial \ln [P_2\text{Glyc}]_{\text{free}}}. \quad (31)$$

Using eqn (31), we can obtain the *free*  $P_2\text{Glyc}$  concentration,

$$[P_2\text{Glyc}]_{\text{free}} = [P_2\text{Glyc}]_{\text{total}} - \tilde{Y}_{P_2\text{Glyc}} [\text{Hb}]. \quad (32)$$

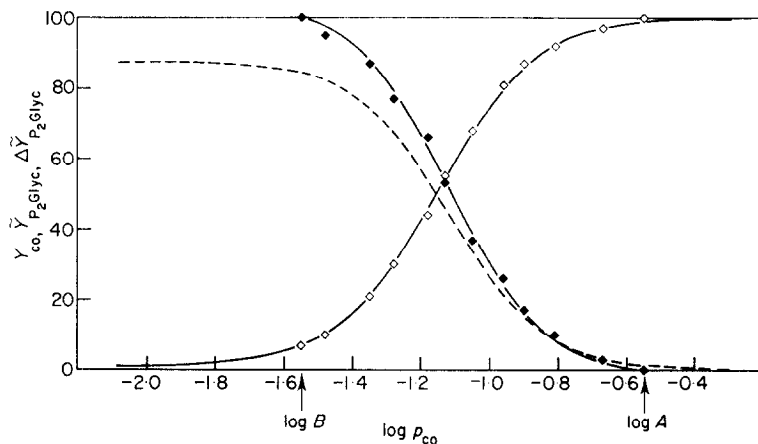


FIG. 4. Experimental measurements (Heustis & Raftery, 1972a) of carbon monoxide binding,  $Y_{\text{CO}}$ , and  $\text{P}_2\text{Glyc}$  binding,  $\bar{Y}_{\text{P}_2\text{Glyc}}$ , under the conditions of  $32^\circ\text{C}$  and pH 7.40 (0.1 M-bis-Tris buffer). The concentration of Hb is  $2 \times 10^{-3}$  M (by tetramer), and the concentration of  $\text{P}_2\text{Glyc}$  is  $3 \times 10^{-3}$  M. Open symbols denote  $Y_{\text{CO}}$ , while closed symbols denote  $\Delta\bar{Y}_{\text{P}_2\text{Glyc}}$ , where  $\Delta\bar{Y}_{\text{P}_2\text{Glyc}}(p_{\text{CO}}) = [\bar{Y}_{\text{P}_2\text{Glyc}}(p_{\text{CO}}) - \bar{Y}_{\text{P}_2\text{Glyc}}(A)] / [\bar{Y}_{\text{P}_2\text{Glyc}}(B) - \bar{Y}_{\text{P}_2\text{Glyc}}(A)]$ . The solid curves represent the best fit of the theoretical expressions developed in the text (see eqns (15) and (28) to (32)). The five parameters used are  $U_q^* = 28$  kT,  $K = 1.9 \times 10^3$  mm Hg $^{-1}$ ,  $U_{qt} = 2.5$  kT,  $\bar{K}_{\text{deoxy}} = 5.46 \times 10^3$  M $^{-1}$ , and  $\bar{K}_{\text{oxy}} = 7.93 \times 10^{-4}$  M $^{-1}$ , where  $k$  is the Boltzmann constant and  $T$  is the temperature in degrees Kelvin ( $kT = 0.0263$  eV at  $32^\circ\text{C}$ ). The broken line represents the theoretical values of  $\bar{Y}_{\text{P}_2\text{Glyc}}$ , from which  $\Delta\bar{Y}_{\text{P}_2\text{Glyc}}$  was calculated.

Figure 4 displays data of Heustis & Raftery (1972a) for  $Y_{\text{CO}}$  and  $\bar{Y}_{\text{P}_2\text{Glyc}}$  as a function of  $p_{\text{CO}}$  at a single value of  $[\text{P}_2\text{Glyc}]_{\text{total}}$ . The solid curves represent the theoretical equilibrium curves obtained from the set of simultaneous equations (15) and (28) to (32) (where  $\text{O}_2$  is replaced by CO in all expressions). The five parameters  $U_q^*$ ,  $U_{qt}$ ,  $K$ ,  $\bar{K}_{\text{deoxy}}$ , and  $\bar{K}_{\text{oxy}}$  of these equations were chosen to achieve a least-squares fit.

Figure 5(a) displays a family of curves, one for each of five discrete values of  $[\text{P}_2\text{Glyc}]_{\text{total}}$ , of  $Y_{\text{O}_2}$  as a function of  $p_{\text{O}_2}$ . The data are from Benesch *et al.* (1969) and Benesch & Benesch (1971, personal communication). The solid curves show the fit of the same five-parameter set of simultaneous equations, (15) and (28) to (32), as was used in fitting the data of Figure 4.

Figure 6(a) represents a family of oxygenation curves analogous to that of Figure 5(a), but for a different set of experimental conditions. These data are from Bunn (1971, unpublished results). The solid curves are obtained by fitting the same five-parameter set of simultaneous equations, (15) and (28) to (32), as was used in Figures 4 and 5(a).

Notice that, for the data in Figures 5 and 6, although  $\bar{K}_{\text{oxy}}$  is much smaller than  $\bar{K}_{\text{deoxy}}$ , it is significantly greater than zero. It is impossible to achieve a satisfactory fit in the full range of the oxygenation data if we assume that  $\bar{K}_{\text{oxy}}$  is zero, as is often done (e.g. Ogata & McConnell, 1972b).

The fits of the theoretical expressions to the data of Figures 5(a) and 6(a) are good except at low oxygenation levels when  $[\text{P}_2\text{Glyc}]_{\text{free}} = 0$ . Thus, it would appear that while most of the effect of  $\text{P}_2\text{Glyc}$  is explained by the assumption that  $\text{P}_2\text{Glyc}$  is a simple quaternary effector, this description may not be entirely complete.

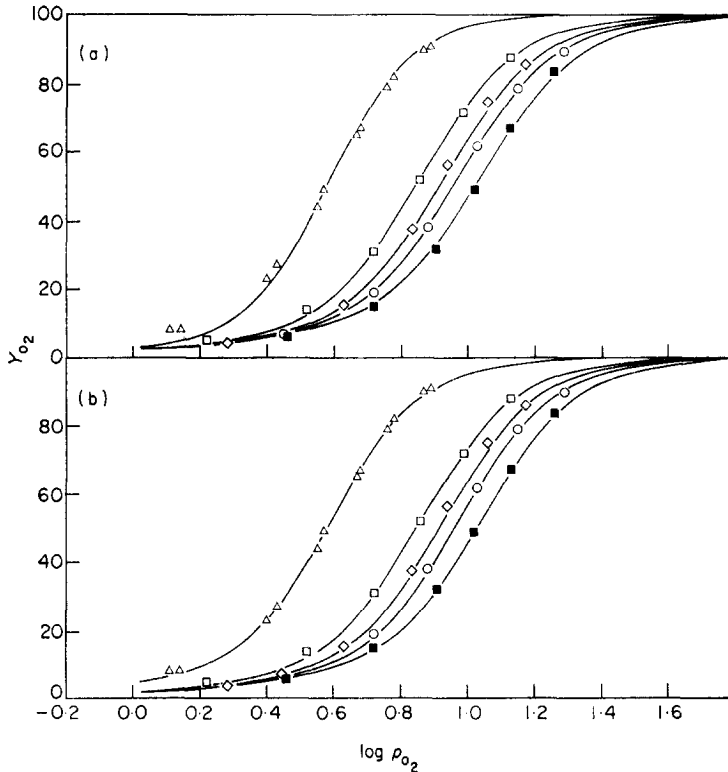


FIG. 5. Experimental oxygenation data at pH 7.3 and 0.1 M-Cl<sup>-</sup>, compared with the theoretical equilibrium curves. Data points taken at 20°C with  $6 \times 10^{-5}$  M-hemoglobin (by tetramer) and 0.05 M-bis-Tris buffer (Benesch *et al.*, 1969; Benesch & Benesch, personal communication). Total P<sub>2</sub>Glyc: ( $\Delta$ ) none; ( $\square$ )  $1.3 \times 10^{-4}$  M; ( $\diamond$ )  $2.5 \times 10^{-4}$  M; ( $\circ$ )  $4.0 \times 10^{-4}$  M; ( $\blacksquare$ )  $1.0 \times 10^{-3}$  M.

(a) Theoretical equilibrium curves shown for the five parameter values:  $U_q^* = 23.0$  kT;  $K = 1.4$  mm Hg<sup>-1</sup>;  $U_{qt} = 2.05$  kT;  $K_{\text{deoxy}} = 1.1 \times 10^5$  M<sup>-1</sup>;  $K_{\text{oxy}} = 1.2 \times 10^3$  M<sup>-1</sup>.

(b) Theoretical equilibrium curves shown for the six parameter values:  $U_q^* = 21.0$  kT;  $K = 1.5$  mm Hg<sup>-1</sup>;  $U_{qt} = 1.85$  kT;  $U'_{qt} = 2.05$  kT;  $K_{\text{deoxy}} = 1.3 \times 10^5$  M<sup>-1</sup>;  $K_{\text{oxy}} = 4.5 \times 10^1$  M<sup>-1</sup>.

### (b) Differences between the $\alpha$ and $\beta$ chains

In the theoretical equations developed thus far, we have assumed that the  $\alpha$  and the  $\beta$  chains of HbA behave identically with respect to substrate binding and molecular constraints. To partially test this hypothesis, we attempted to obtain better fits to the experimental data by developing theoretical equations allowing for differences between the  $\alpha$  and  $\beta$  chains.

The data in Figure 7 (Heustis & Raftery, 1972b) show that oxygen binding to the  $\beta$  chains lags oxygen binding to the  $\alpha$  chains. This difference between the  $\alpha$  and  $\beta$  subunits can be taken into account by deriving the generalization of eqn (28) for the situation in which the oxygen binding constants  $K_{\text{oxy}}$  and  $K_{\text{deoxy}}$  are different for the  $\alpha$  and  $\beta$  subunits. We find, by the same methods used above, that

$$Z = (1 + \tilde{K}_{\text{deoxy}}[\text{P}_2\text{Glyc}]_{\text{free}})(1 + K_{\text{deoxy}}^{\alpha} p_{\text{O}_2})(1 + K_{\text{deoxy}}^{\beta} p_{\text{O}_2})^2 + (1 + \tilde{K}_{\text{oxy}}[\text{P}_2\text{Glyc}]_{\text{free}}) \exp(-U_q^*/kT) (1 + K_{\text{oxy}}^{\alpha} p_{\text{O}_2})^2 (1 + K_{\text{oxy}}^{\beta} p_{\text{O}_2})^2, \quad (33a)$$

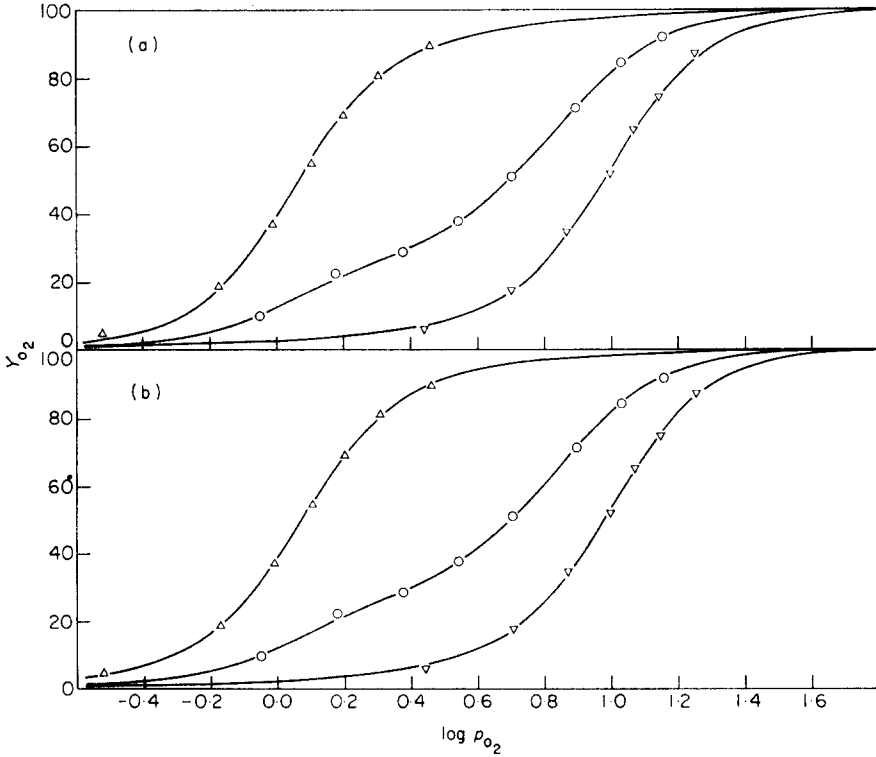


FIG. 6. Experimental oxygenation data at pH 7.25 and 0.01 M-Cl<sup>-</sup>, compared with the theoretical equilibrium curves. Data points taken at 20°C with 1.17 × 10<sup>-4</sup> M-hemoglobin (by tetramer) and bis-Tris buffer (Bunn, unpublished results). Total P<sub>2</sub>Glyc: (Δ) none; (○) 8.62 × 10<sup>-5</sup> M; (∇) 1.15 × 10<sup>-3</sup> M.

(a) Theoretical equilibrium curves shown for the five parameter values:  $U_q^* = 6.2 kT$ ;  $K = 0.30$  mm Hg<sup>-1</sup>;  $U_{qt} = 1.25 kT$ ;  $K_{deoxy} = 1.2 \times 10^7$  M<sup>-1</sup>;  $K_{oxy} = 3.9 \times 10^3$  M<sup>-1</sup>.

(b) Theoretical equilibrium curves shown for the six parameter values:  $U_q^* = 7.8 kT$ ;  $K = 0.81$  mm Hg<sup>-1</sup>;  $U_{qt} = 1.0 kT$ ;  $U'_{qt} = 1.75 kT$ ;  $K_{deoxy} = 1.5 \times 10^7$  M<sup>-1</sup>;  $K_{oxy} = 1.2 \times 10^3$  M<sup>-1</sup>.

where here

$$U_q^* = U_q + 4U_{qt}^\alpha + 4U_{qt}^\beta. \tag{33b}$$

Here we have defined

$$K_{deoxy}^\alpha \equiv \exp(-2U_{qt}^\alpha/kT) \times K^\alpha \tag{34a}$$

$$K_{oxy}^\alpha \equiv \exp(2U_{qt}^\alpha/kT) \times K^\alpha \tag{34b}$$

$$K_{deoxy}^\beta \equiv \exp(-2U_{qt}^\beta/kT) \times K^\beta \tag{34c}$$

$$K_{oxy}^\beta \equiv \exp(2U_{qt}^\beta/kT) \times K^\beta, \tag{34d}$$

where  $K^\alpha$  and  $K^\beta$  are straightforward generalizations for the  $\alpha$  and  $\beta$  chains of the quantity  $K$  defined in eqn (15c),

$$p_{O_2} K^\alpha \equiv \exp(\mu_{O_2}/kT) \exp(-(U_\emptyset^\alpha + U_{\emptyset t}^\alpha + U_t^\alpha)/kT) \tag{34e}$$

$$p_{O_2} K^\beta \equiv \exp(\mu_{O_2}/kT) \exp(-(U_\emptyset^\beta + U_{\emptyset t}^\beta + U_t^\beta)/kT). \tag{34f}$$

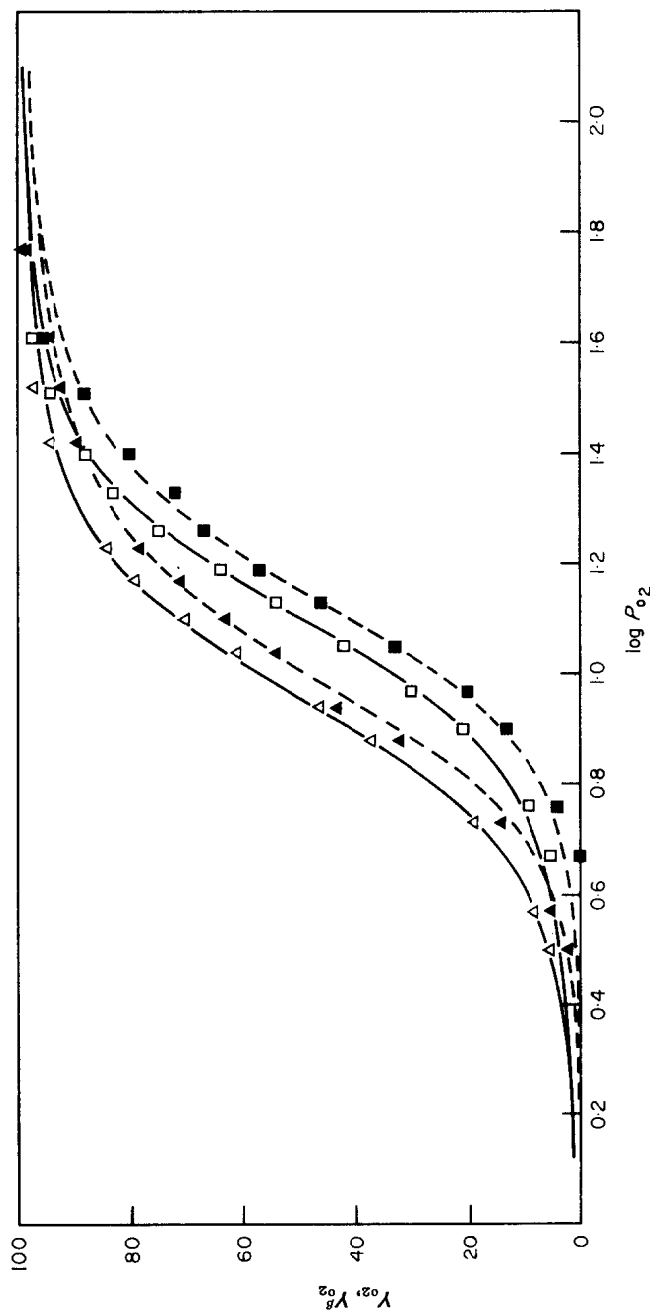


FIG. 7. Experimental measurements (Heustis & Raftery, 1972b) of percentage oxygenation of hemoglobin ( $Y_{O_2}$ ) and percentage oxygenation of the  $\beta$  chains ( $Y_{O_2}^\beta$ ). The data are taken under conditions of  $0.1 \text{ M-Cl}^-$ ,  $15^\circ\text{C}$ ,  $2 \times 10^{-3} \text{ M-hemoglobin}$  (by tetramer), and pH 7.25 ( $0.1 \text{ M-bis-Tris}$  buffer). The open symbols denote  $Y_{O_2}$  while the closed symbols denote  $Y_{O_2}^\beta$ . The symbol ( $\Delta$ ) represents data taken in the absence of  $\text{P}_2\text{Glyc}$ , while ( $\square$ ) represents data taken with a total  $\text{P}_2\text{Glyc}$  concentration of  $4 \times 10^{-3} \text{ M}$ . The curves represent the best fit of the theoretical expressions derived in the text for inequivalent  $\alpha$  and  $\beta$  chains (see eqns (15) and (29) to (35)). The solid curves represent the theoretical values of  $Y_{O_2}$  while the broken curves represent the theoretical values of  $Y_{O_2}^\beta$ .

The seven parameter values used here are  $U_q^* = 8.34 \text{ kT}$ ,  $K^\alpha = 0.324 \text{ mm Hg}^{-1}$ ,  $K^\beta = 0.0158 \text{ mm Hg}^{-1}$ ,  $U_q^\alpha = 1.45 \text{ kT}$ ,  $U_q^\beta = 1.61 \text{ kT}$ ,  $\tilde{K}_{\alpha\text{oxy}} = 3.83 \times 10^5 \text{ M}^{-1}$ , and  $\tilde{K}_{\beta\text{oxy}} = 1.12 \times 10^5 \text{ M}^{-1}$ .

Applying eqn (30), we find the expected result that the fraction of heme groups oxygenated is equal to the average of the fraction of  $\alpha$  chains oxygenated and the fraction of the  $\beta$  chains oxygenated,

$$Y_{O_2} = \frac{1}{4} \left[ \frac{\partial \ln Z}{\partial \ln p_{O_2}} \right] = \frac{1}{4} \left[ \frac{\partial \ln Z}{\partial \ln K^\alpha} + \frac{\partial \ln Z}{\partial \ln K^\beta} \right] = \frac{1}{2} [Y^\alpha_{O_2} + Y^\beta_{O_2}] \quad (35a)$$

where

$$Y^\alpha_{O_2} = \frac{1}{2} \frac{\partial \ln Z}{\partial \ln K} K^\alpha \quad (35b)$$

and

$$Y^\beta_{O_2} = \frac{1}{2} \frac{\partial \ln Z}{\partial \ln K} K^\beta. \quad (35c)$$

The curves in Figure 7 are obtained from the theoretical equations (15) and (29) to (35), where the seven parameters  $U^*_q$ ,  $K^\alpha$ ,  $K^\beta$ ,  $U^*_{qt}$ ,  $U^B_{qt}$ ,  $\tilde{K}_{deoO_2}$ , and  $\tilde{K}_{oxy}$  have been varied to obtain a least-squares fit. We find that the strength of the molecular

TABLE 1

*Summary of the parameter values used to obtain the solid (theoretical) curves in Figures 4, 5(a), 6(a) and 7*

	Fig. 4	Fig. 5(a)	Fig. 7		Fig. 6(a)
pH	7.40	7.30	7.25		7.25
Cl <sup>-</sup> (M)	0.1	0.1	0.1		0.01
Temperature (°C)	32	20	15		20
$kT$ (eV)	0.0263	0.0244	0.0240		0.0244
Hb (M)	$2 \times 10^{-3}$	$6 \times 10^{-5}$	$2 \times 10^{-3}$		$1.17 \times 10^{-4}$
bis-Tris (M)	0.05	0.05	0.1		—
			$\alpha$	$\beta$	
$K$	$1.9 \times 10^2$ per mm Hg of CO	1.4 per mm Hg of O <sub>2</sub>	0.324 per mm Hg of O <sub>2</sub>	0.0158 per mm Hg of O <sub>2</sub>	0.30 per mm Hg of O <sub>2</sub>
$U^*_{qt}$ ( $kT$ )	2.5	2.1	1.45	1.61	1.3
$U^*_q$ ( $kT$ )	23	23	8.3		6.2
$\tilde{K}_{deoO_2}$ (M <sup>-1</sup> )	$5.46 \times 10^3$	$1.1 \times 10^5$	$3.83 \times 10^5$		$1.2 \times 10^7$
$\tilde{K}_{oxy}$ (M <sup>-1</sup> )	( $7.93 \times 10^{-4}$ )	( $1.2 \times 10^3$ )	(1.12 × 10 <sup>5</sup> )		( $3.9 \times 10^3$ )

Decreasing pH seems to shift the tertiary equilibrium toward the deoxy conformation (i.e. decrease  $K$ ), weaken the molecular constraints (i.e. decrease  $U^*_{qt}$ ), and shift the quaternary equilibrium toward the oxy conformation (i.e. decrease  $U^*_q$ ). Thus hydrogen ion appears to act as a tertiary effector, a constraint effector, and a quaternary effector. This multiplicity of effects is not surprising in view of the fact that there are a very large number of possible H<sup>+</sup> binding sites on a large protein molecule.

Binding of P<sub>2</sub>Glyc to the deoxy quaternary structure is weakened (i.e.  $\tilde{K}_{deoO_2}$  is decreased) by higher Cl<sup>-</sup> concentrations and higher values of pH, as was observed by Benesch *et al.* (1969). Thus Cl<sup>-</sup> and H<sup>+</sup> are second-order quaternary effectors. Cl<sup>-</sup> may be a quaternary effector competing with P<sub>2</sub>Glyc. H<sup>+</sup>, by protonating acid groups, facilitates P<sub>2</sub>Glyc binding.

The binding of P<sub>2</sub>Glyc to the oxy quaternary structure is very weak (i.e.  $\tilde{K}_{oxy}$  is very small). Since very little of the hemoglobin in the oxy quaternary conformation has P<sub>2</sub>Glyc bound, the fit of the theoretical curves to the oxygenation data is not very sensitive to the value of  $\tilde{K}_{oxy}$  so that the values of  $\tilde{K}_{oxy}$  shown in the Table are not very accurate. (For this reason we enclose them in parentheses.)

constraints on the  $\alpha$  and  $\beta$  chains appear to be approximately equal (i.e.  $U_{qt}^\alpha \cong U_{qt}^\beta$ ). However, the oxygen binding affinity is higher for the  $\alpha$  subunits than for the  $\beta$  subunits (i.e.  $K^\alpha > K^\beta$ ). (The parameters of the theoretical curves shown in Figs 4, 5(a), 6(a), and 7 are summarized and discussed further in Table 1.)

Notice that in eqn (33) (as in eqn (28)) the strength of P<sub>2</sub>Glyc binding depends only on the quaternary structure of the hemoglobin molecule. Although P<sub>2</sub>Glyc is thought to bind to acid groups of the  $\beta$  chains (Bunn & Briehl, 1970; Bauer, 1970; Tomita & Riggs, 1971; Caldwell *et al.*, 1971), the positions of these particular groups—and hence the P<sub>2</sub>Glyc binding affinity—seem to depend primarily on the quaternary conformation of the molecule rather than on the tertiary conformations of the individual  $\beta$  chains.

We find that the expression for  $Z$  given by eqn (33), which results in a theoretical expression for  $Y_{O_2}$  with seven adjustable parameters, does not produce better agreement with the data of Figures 5 and 6 than the earlier expression for  $Z$ , given by eqn (28), which involves only five adjustable parameters. Thus, we infer that the difference between the oxygen affinities of the  $\alpha$  and  $\beta$  subunits is not important in the effect of P<sub>2</sub>Glyc on the oxygen equilibrium of HbA.

### (c) 2,3-Diphosphoglycerate as a constraint effector

In eqns (28) and (33), we have assumed that P<sub>2</sub>Glyc is purely a quaternary effector. However, P<sub>2</sub>Glyc may also change the strength of the molecular constraints. In fact, if we consider P<sub>2</sub>Glyc as a constraint effector as well as a quaternary effector, we can fit the data of Figures 5 and 6 very well. Instead of the five parameters of eqn (28), or the seven parameters of eqn (33), we have the six-parameter equation

$$Z = \{(1 + K_{\text{deoxy}} p_{O_2})^4 + \exp(-U_q^*/kT)(1 + K_{\text{oxy}} p_{O_2})^4\} + [\text{P}_2\text{Glyc}]_{\text{free}} \{\tilde{K}_{\text{deoxy}}(1 + K'_{\text{deoxy}} p_{O_2})^4 + \tilde{K}_{\text{oxy}} \exp(-U_q^*/kT)(1 + K'_{\text{oxy}} p_{O_2})^4\} \quad (36)$$

where

$$K'_{\text{deoxy}} \equiv \exp(-2U'_{qt}/kT) \times K \quad (37a)$$

and

$$K'_{\text{oxy}} \equiv \exp(2U'_{qt}/kT) \times K. \quad (37b)$$

The added parameter,  $U'_{qt}$ , is the strength of the q-t interaction when P<sub>2</sub>Glyc is bound, while  $U_{qt}$  is the strength of the q-t interaction in the absence of P<sub>2</sub>Glyc:

$$U'_{qt} = U_{qt} + U_{\bar{q}qt}. \quad (37c)$$

Note that the strength of P<sub>2</sub>Glyc binding to each conformation now depends on the level of oxygenation.  $\tilde{K}_{\text{deoxy}}$  and  $\tilde{K}_{\text{oxy}}$  represent the constants for P<sub>2</sub>Glyc binding to the deoxy and oxy quaternary conformations, respectively, when no oxygen is present.

The six-parameter set of simultaneous equations (29) to (32), (36), (37) and (15) described the data nicely, as shown in Figures 5(b) and 6(b), indicating that P<sub>2</sub>Glyc binding not only shifts the quaternary equilibrium ( $\tilde{K}_{\text{deoxy}} > \tilde{K}_{\text{oxy}}$ ) but also increases molecular constraints ( $U'_{qt} > U_{qt}$ ). This second effect may be related to the distortion of HbA by P<sub>2</sub>Glyc binding which has been observed by Arnone (1972).

Notice that with six adjustable parameters, three of the six degrees of freedom are determined by one curve at one P<sub>2</sub>Glyc concentration and the other three by another curve at a second P<sub>2</sub>Glyc concentration. Thus, from just two curves we can get enough information to predict any number of additional curves at any other

$P_2$ Glyc concentrations. However, by fitting a large number of curves at once, we obtained more accurate values for the theoretical parameters.

Notice also that  $p_{1/2}$  is fit as well in Figures 5(a) and 6(a) as in Figures 5(b) and 6(b). It is necessary to consider the  $P_2$ Glyc dependence of the *full* oxygenation curve in order to detect the constraint effect of  $P_2$ Glyc.

(d) *The quaternary equilibrium*

The foregoing analysis is based on the Perutz picture. This assumes that the tertiary conformation of a subunit changes when oxygen binds (induced-fit binding). However, no assumption is made about the change in quaternary conformation. By fitting oxygenation data, we have obtained parameter values which *fully* describe the system and allow us to calculate the probability of each microscopic state of the system. In particular, we can calculate the probability that a hemoglobin molecule with  $n$  heme sites oxygenated will be in one or the other of the two quaternary conformations (Herzfeld & Stanley, 1972*a,b*). The results of such calculations, using the parameter values found for the data of Figures 5 and 6, are shown in Figure 8(a) and 8(b) respectively. The predictions that the switch from the deoxy to the oxy quaternary conformation occurs at about the third oxygenation and that it is not very sensitive to  $P_2$ Glyc concentration are in rough agreement with the observations of Hopfield *et al.* (1972), Gibson & Parkhurst (1968), and Salhany *et al.* (1972).

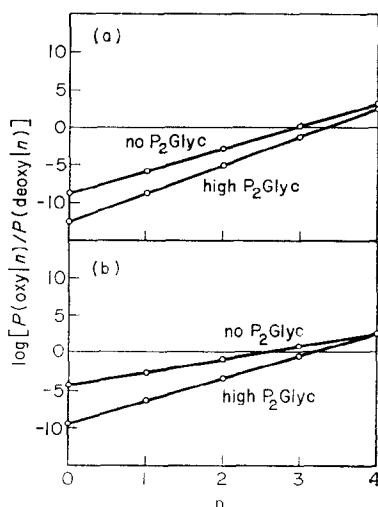


FIG. 8. Theoretical calculation of the relative probabilities of the oxy and deoxy quaternary conformations in a hemoglobin molecule with  $n$  hemes oxygenated ( $P(\text{oxy}|n)$  and  $P(\text{deoxy}|n)$ , respectively). (a) Calculations based on the theoretical parameters of Fig. 5(b), for the conditions of pH 7.3, 0.1 M-Cl<sup>-</sup> and 20°C. (b) Calculations based on the theoretical parameters of Fig. 6(b), for the conditions of pH 7.25, 0.01 M-Cl<sup>-</sup> and 20°C.

Since the quaternary conformation switches from deoxy to oxy approximately when the third oxygen molecule binds to hemoglobin, and since  $P_2$ Glyc binds very strongly to the deoxy quaternary conformation but only very weakly to the oxy conformation, it follows that  $P_2$ Glyc is released at about the third oxygenation. This conclusion is consistent with the observation of Heustis & Raftery (1972*a*) that the fraction of HbA molecules *without*  $P_2$ Glyc bound is roughly equal to the

fraction of molecules with four hemes liganded plus about half of the fraction with three hemes liganded. Heustis & Raftery have interpreted this data as supporting the theory that the  $\alpha$  chains are oxygenated first and that P<sub>2</sub>Glyc is released when the  $\beta$  chains are oxygenated. However, we have shown here that these data can be explained even if the  $\alpha$  and  $\beta$  chains are assumed to be equivalent, and if P<sub>2</sub>Glyc is only released when the quaternary conformation changes from deoxy to oxy.

(e) *2,3-Diphosphoglycerate dependence of the Adair parameters and apparent free energy of interaction*

Eqn (36)—or any other partition function for HbA—can be rewritten in the Adair form (Adair, 1925*a,b*)

$$Z = 1 + 4k_1 p_{O_2} + 6k_1 k_2 p_{O_2}^2 + 4k_1 k_3 k_2 p_{O_2}^3 + k_1 k_2 k_3 k_4 p_{O_2}^4. \quad (38)$$

Thus we can obtain explicit expressions for the dependence of the Adair constants,  $k_1$ – $k_4$ , and the apparent free energy of interaction  $\Delta F = RT \ln (k_4/k_1)$  (Whitehead, 1970), upon the *free* P<sub>2</sub>Glyc concentration. The results of such calculations are shown in Figure 9. In Figure 9(a), we see that, in general, increasing the free P<sub>2</sub>Glyc concentration decreases the four Adair constants; however, at low ionic strength (0.01 M-Cl<sup>-</sup>),  $k_4$  is nearly independent of P<sub>2</sub>Glyc. Tyuma *et al.* (1971) have calculated  $k_1$  to  $k_4$  for only *two* P<sub>2</sub>Glyc concentrations in 0.01 M-Cl<sup>-</sup>. They found that at this low ionic strength the values of  $k_1$  to  $k_3$  decrease when the P<sub>2</sub>Glyc concentration is increased, while the value of  $k_4$  is apparently unaffected by the change in P<sub>2</sub>Glyc concentration. Thus their results are entirely consistent with ours. The effect of P<sub>2</sub>Glyc on  $k_1$  is particularly significant. If P<sub>2</sub>Glyc were not a constraint effector,  $k_1$  would be unaffected by P<sub>2</sub>Glyc concentration. The fact that  $k_1$  is observed to decrease with increasing P<sub>2</sub>Glyc concentration is proof that P<sub>2</sub>Glyc is not exclusively a quaternary effector.

Roughton & Lyster (1965) have measured  $\Delta F$  at pH 7.0 and high ionic strength. Their value of 2.71 kcal/mol is in good agreement with our calculated values.

(f) *Biphasic oxygenation curves*

Biphasic-shaped oxygenation curves (such as the one shown in Fig. 6) are easily understood in the light of the P<sub>2</sub>Glyc-dependence of the Adair constants. As oxygen binds, the hemoglobin quaternary equilibrium shifts toward the oxy conformation and, since P<sub>2</sub>Glyc has less affinity for the oxy conformation, bound P<sub>2</sub>Glyc is released. Therefore, only when the *total* P<sub>2</sub>Glyc concentration is either zero or much larger than the hemoglobin concentration can the *free* P<sub>2</sub>Glyc concentration be considered to remain constant during oxygenation. On the other hand, when the total P<sub>2</sub>Glyc concentration is *comparable* to the hemoglobin concentration, the free P<sub>2</sub>Glyc concentration increases significantly during oxygenation. If this P<sub>2</sub>Glyc increase occurs within certain ranges of P<sub>2</sub>Glyc concentrations, it will cause a sharp decrease in one (or more) of the Adair constants, as shown in Figure 9. A plateau will appear in the oxygenation curve where this sharp decrease in binding affinity occurred, giving rise to the characteristic biphasic shape.

Tomita & Riggs (1971) have observed that for mouse hemoglobin the Hill coefficient,  $n_H$ , varies as the ratio of P<sub>2</sub>Glyc to Hb increases;  $n_H$  decreases to a minimum when the ratio is one, and gradually returns to normal as the ratio becomes large. This dip in  $n_H$  probably corresponds to the flattening of the middle part of the biphasic

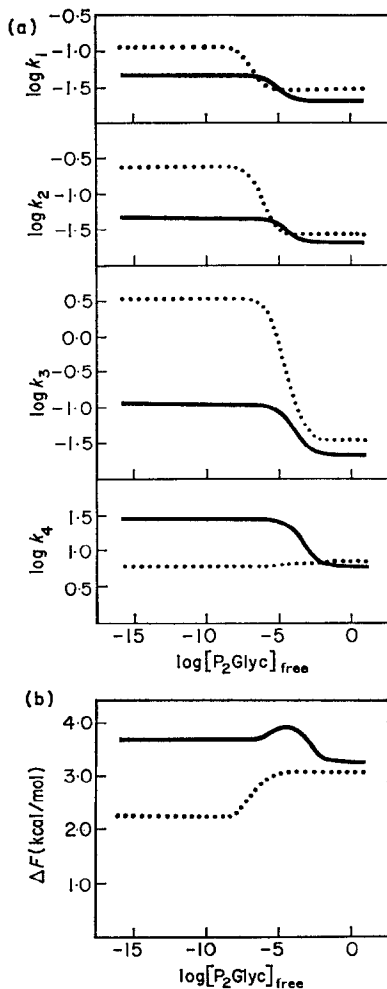


FIG. 9. The dependence of (a) the Adair parameters and (b) the apparent free energy of interaction on the free  $P_2Glyc$  concentration. The solid curve represents calculations based on the theoretical parameters of Fig. 5(b), for the conditions of pH 7.3,  $0.1 \text{ M-Cl}^-$ , and  $20^\circ\text{C}$ . The dotted curve represents calculations based on the theoretical parameters of Fig. 6(b), for the conditions of pH 7.25,  $0.01 \text{ M-Cl}^-$ , and  $20^\circ\text{C}$ .

oxygenation curves. Since chloride and other phosphate ions diminish the effect of  $P_2Glyc$ , it is not surprising that Tomita & Riggs found that the dip in  $n_H$  is less pronounced when these ions are present. Since the strength of  $P_2Glyc$  binding in the deoxy quaternary conformation is strongly dependent on protonation of acid groups in the central cavity of Hb (i.e. hydrogen ions are second-order quaternary effectors), it is also not surprising that Tomita & Riggs found the dips in  $n_H$  become smaller as pH increases above 6.0, and that these dips disappear altogether above pH 8.0. Thus the pH dependence of  $n_H$  may be the result of the second-order quaternary effect of  $H^+$ , and may be expected to be strongest where the effect of  $P_2Glyc$  on  $n_H$  is strongest (i.e. at low ionic strengths, with a  $P_2Glyc:Hb$  ratio of about unity).

## 6. Dissociation of Hemoglobin

(a) *HbA*

The analysis of sections 3 to 5 has assumed that the HbA tetramer does not dissociate. However, at very dilute concentrations, HbA does dissociate, as evidenced by the dependence of the oxygenation curve on hemoglobin concentration (see the data of Thomas & Edelstein, 1972 in Fig. 10). In order to account for dissociation, it is necessary to add to eqn (5) an energy term of the form

$$\delta\mathcal{E} = -N\mu_p + U_N, \quad (39)$$

where  $\mu_p$  is the chemical potential of *unliganded* hemoglobin subunits, and  $U_N$  is the energy of aggregation of  $N$  *unliganded* subunits.

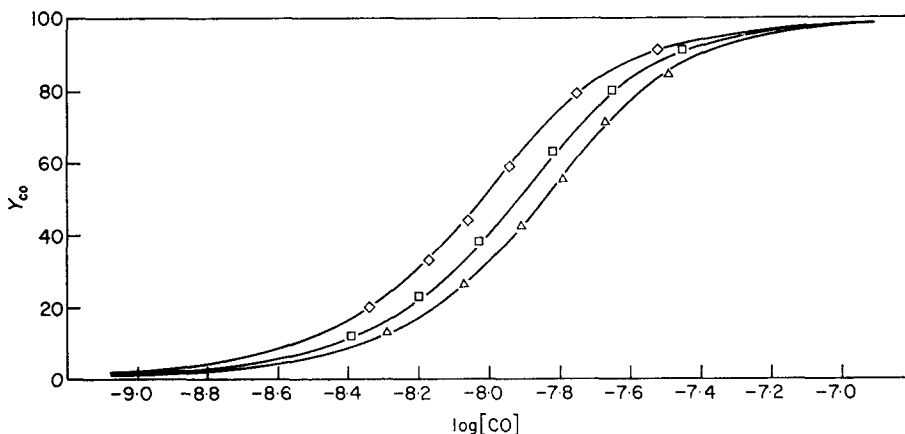


FIG. 10. Experimental measurements (Thomas & Edelstein, 1972) of carbon monoxide binding,  $Y_{CO}$ , as a function of the concentration of CO. Data are taken at pH 7.0 and 24°C, in 2 M-NaCl and 0.1 M- $K_2PO_4$  buffer. Three values of hemoglobin concentration (by tetramer) are shown: ( $\diamond$ )  $3.0 \times 10^{-8}$  M, ( $\square$ )  $8.0 \times 10^{-8}$  M, and ( $\triangle$ )  $1.6 \times 10^{-7}$  M. The solid curves are obtained from a best fit of eqns (42), (44), (47) and (48) of section 6. They utilize the five parameter values  $K_{dimer} = 4.68 \times 10^8$  M $^{-1}$ ,  $K_A = 6.72 \times 10^9$  M $^{-1}$ ,  $U_q^* = 2.05$  kT,  $K = 3.18 \times 10^8$  M $^{-1}$  and  $U_{qt} = 2.31$  kT. The  $P_2$ Glyco concentration is assumed to be negligible (i.e. much smaller than  $K_{deoxy}^{-1}$ , where  $K_{deoxy}$  is small because of the high  $Cl^-$  and  $PO_4^-$  concentration).

The calculation follows as before, with the result that

$$Z = C_1 Z_I + K_{II} C_1^2 Z_{II} + K_{IV} C_1^4 Z_{IV} \quad (40)$$

for a tetramer that dissociates into dimers and monomers. Here,  $C_1$  is the concentration of *unliganded* monomer, and  $Z_I$ ,  $Z_{II}$ , and  $Z_{IV}$  are the partition functions for the protein molecules composed of 1, 2, and 4 subunits, respectively. The association constants  $K_{II}$  and  $K_{IV}$  are given by

$$K_{II} C_1^2 = \exp(2\mu_p/kT) \exp(-U_2/kT) \quad (41a)$$

and

$$K_{IV} C_1^4 = \exp(4\mu_p/kT) \exp(-U_4/kT). \quad (41b)$$

For HbA,  $Z_{IV}$  is given by the expression

$$Z_{IV} = (1 + K_{deoxy} p_{O_2})^4 + \exp(-U/kT)(1 + K_{oxy} p_{O_2})^4 \quad (42a)$$

(cf. eqn 13).

For non-co-operative dimers,

$$Z_{II} = (1 + K_{dimer} p_{O_2})^2, \quad (42b)$$

and for the monomer, we have simply

$$Z_I = (1 + K_{monomer} p_{O_2}). \quad (42c)$$

The fraction of hemes oxygenated is given by an expression analogous to eqn (30),

$$Y_{O_2} = \left( \frac{\partial \ln Z}{\partial \ln p_{O_2}} \right) / \left( \frac{\partial \ln Z}{\partial \ln C_1} \right). \quad (43)$$

For HbA,  $K_{II}$  and  $K_{IV}$  are very large so that at hemoglobin concentrations as high as those used in Figure 10, essentially no monomer is present. Therefore, we have effectively

$$\begin{aligned} Z &= K_{II} C_1^2 Z_{II} + K_{IV} C_1^4 Z_{IV} \\ &= C_2 Z_{II} + K_A C_2^2 Z_{IV}. \end{aligned} \quad (44)$$

Here  $C_2$  is the concentration of unliganded dimer,

$$C_2 = K_{II} C_1^2, \quad (45)$$

and  $K_A$  is the association constant for aggregation of unliganded dimers into unliganded tetramers,

$$K_A = \frac{K_{IV}}{K_{II}^2}. \quad (46)$$

Instead of eqn (43) for the fraction of hemes oxygenated, we can use eqn (45) to obtain the equation

$$Y_{O_2} = \left( \frac{\partial \ln Z}{\partial \ln p_{O_2}} \right) / \left( 2 \frac{\partial \ln Z}{\partial \ln C_2} \right). \quad (47)$$

Note that  $C_2$  is given by the solution of the quadratic equation

$$C = 2C_2 Z_{II} + 4K_A C_2^2 Z_{IV}, \quad (48)$$

where  $C$  represents the total concentration of subunits (liganded or unliganded, aggregated or not).

The five parameters of the set of simultaneous equations (42), (44), (47) and (48) have been fit to the carbon monoxide binding data of Figure 10 (one must replace the symbol  $p_{O_2}$  by [CO] in all the equations). From these five parameters, we can calculate an apparent dissociation constant,  $K_D$ , for the HbA tetramer,

$$K_D = \frac{(C_2 Z_{II})^2}{K_A C_2^2 Z_{IV}} = \frac{(1 + K_{dimer} p_{O_2})^4}{K_A [(1 + K_{deoxy} p_{O_2})^4 + \exp(-U_q/kT)(1 + K_{oxy} p_{O_2})^4]}. \quad (49)$$

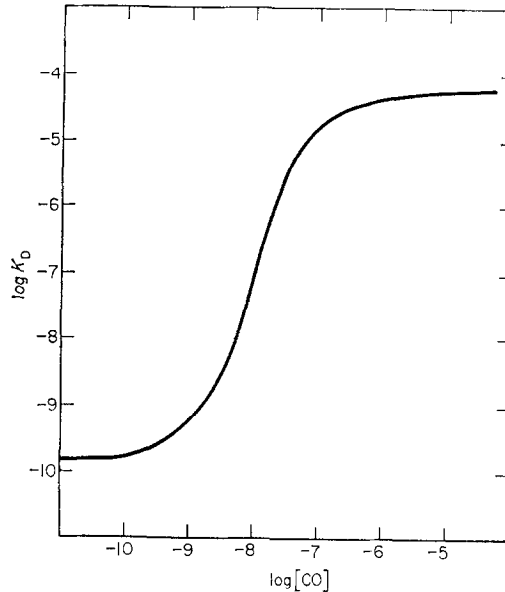


FIG. 11. The apparent dissociation constant,  $K_D$ , of the HbA tetramer as a function of  $[CO]$ , the concentration of carbon monoxide. This calculated curve, based on eqn (49), uses the same five parameters utilized in generating the solid curves of Fig. 10.

As shown in Figure 11, when the CO concentration increases, the apparent dissociation constant increases sharply. Similarly, it has been observed that oxygenated hemoglobin is much more highly dissociated than deoxygenated Hb (Edelstein *et al.*, 1970; Kellett & Gutfreund, 1970; Kellett, 1971). We conclude (cf. eqn (49)) that this sharp increase in dissociation is primarily due to the very high CO affinity of the dimer (since  $K_{dimer}$  is larger than  $K_{oxy}$  or  $K_{deoxy}$ ) rather than the small difference in the stabilities of the two quaternary conformations of the tetramer (as some have postulated).

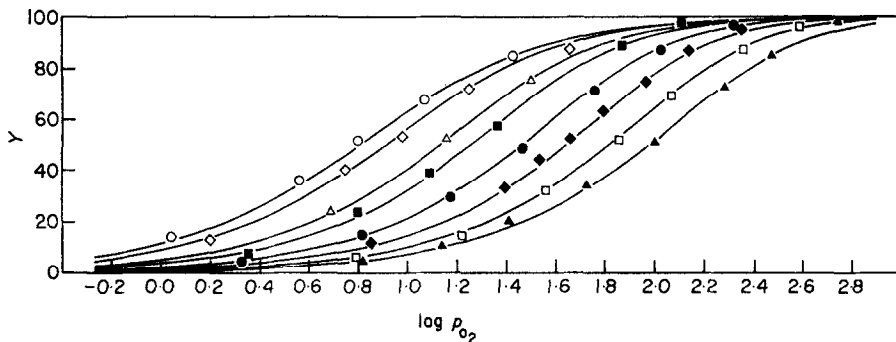


FIG. 12. Experimental data (Briehl, 1963) of the fraction of oxygenated heme sites as a function of partial pressure of oxygen for the sea lamprey, *P. marinus*. The data are taken at 25°C and pH 6.8, in 0.1 M- $K_2PO_4$  buffer. The values of heme concentration (expressed as a multiple of the concentration,  $x$ , of a standard solution—cf. Briehl, 1963) are the following: (○) 2.22 $x$ , (◇) 4.44 $x$ , (△) 15.6 $x$ , (■) 29.0 $x$ , (●) 73.0 $x$ , (◆) 151.0 $x$ , (□) 290.0 $x$ , and (▲) 535.0 $x$ . The solid curves were all obtained from the following set of parameter values:  $K_{monomer} = 2.75 \times 10^{-1}$  mm Hg $^{-1}$ ,  $K = 8.22 \times 10^{-1} x^{-1}$ ,  $K_{dimer} = 2.95 \times 10^{-6}$  mm Hg $^{-1}$ ,  $K_{IV} = 3.53 \times 10^{-3} x^{-3}$ ,  $K_{tetramer} = 2.08 \times 10^{-3}$  mm Hg $^{-1}$ .

(b) *Lamprey hemoglobin*

Dissociation is also important in the oxygenation of lamprey hemoglobin; the data of  $Y_{O_2}$  versus  $p_{O_2}$  of Briehl (1963) are shown in Figure 12. Here the monomer concentration is significant and the concentration of unliganded monomer,  $C_1$ , is given by the solution of the equation

$$C = C_1 Z_I + 2K_{II} C_1^2 Z_{II} + 4K_{IV} C_1^4 Z_{IV}. \tag{50}$$

The seven parameters of the set of simultaneous equations (40), (42), (43) and (50) were fit to the data of Briehl. An equally good fit was obtained with just five parameters by assuming that the tetramer is non-co-operative, so that eqn (42) may be replaced by

$$Z_{IV} = (1 + K_{tetramer} p_{O_2})^4. \tag{51}$$

The theoretical curves for this five-parameter fit to the Briehl data are shown in Figure 12. From this set of parameters, we can determine the fraction  $F_I$  of the hemoglobin molecules which are monomers,

$$F_I = \frac{C_1 Z_I}{Z}, \tag{52a}$$

the fraction  $F_{II}$  which are dimers,

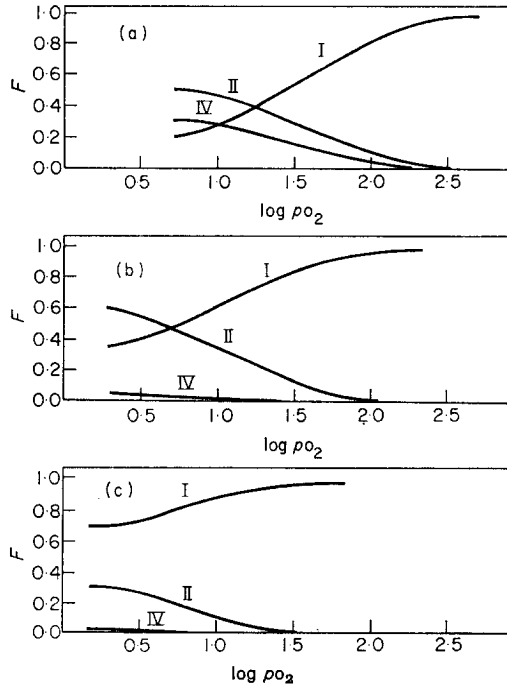


FIG. 13. Predicted curves for the fraction of lamprey hemoglobin molecules that are monomers (curves labeled I), dimers (II), and tetramers (IV). The calculation, based on eqn (52), uses the same set of five parameters as was used in Fig. 12. Curves are shown for the following three heme concentrations (expressed as a multiple of the concentration,  $x$ , of a standard solution—cf. Briehl, 1963): (a)  $290 \cdot 0x$ , (b)  $29 \cdot 0x$ , and (c)  $4 \cdot 44x$ .

$$F_{II} = \frac{K_{II} C_1^2 Z_{II}}{Z}, \quad (52b)$$

and the fraction  $F_{IV}$  which are tetramers,

$$F_{IV} = \frac{K_{IV} C_1^4 Z_{IV}}{Z}, \quad (52c)$$

as functions of the oxygen pressure and the total heme concentration. The results of such calculations are shown in Figure 13.

## 7. Temperature Dependence

In eqn (3) temperature dependence is included explicitly through the presence of the Boltzmann factor,  $1/kT$ . Some additional temperature dependence is also implicit in the terms comprising the energy  $\mathcal{E}$  at most effector concentrations (cf. section 4), unless effector binding has already been explicitly accounted for. For human hemoglobin, we have considered  $P_2$ Glyc binding explicitly (cf. section 5). However, there exist many effectors of oxygenation of human hemoglobin, and so some temperature dependence in  $\mathcal{E}$  is difficult to avoid.

On the other hand, the myoglobin of the mollusc *Buccinum undatum* appears to have very few effectors (Terwilliger & Read, 1971). The sigmoid oxygenation curve is essentially independent of pH,  $P_2$ Glyc, and other phosphates, and it is only weakly affected by chloride ions. Oxygenation is also independent of the myoglobin concentration in the range  $3 \times 10^{-5}$  M to  $1.8 \times 10^{-4}$  M, indicating that the dimers do not dissociate or associate appreciably at these concentrations.

If co-operativity in mollusc myoglobin dimer follows the MWC or Perutz model, then, by analogy with eqn (13), we have

$$Z_{\text{MWC/Perutz}} = [1 + p_{O_2} K_{\text{deoxy}}]^2 + \exp(-U_q^*/kT)[1 + p_{O_2} K_{\text{oxy}}]^2. \quad (53)$$

The binding constants  $K_{\text{deoxy}}$  and  $K_{\text{oxy}}$  are products of a temperature-dependent factor and a temperature-independent constant,

$$K_{\text{deoxy}} = C \exp(-U_{\text{deoxy}}/kT) \quad (54a)$$

$$K_{\text{oxy}} = C \exp(-U_{\text{oxy}}/kT). \quad (54b)$$

However, if the co-operativity is described by the Koshland model, then

$$Z_{\text{Koshland}} = 1 + 2[\exp(-2U_{tt}/kT)K]p_{O_2} + K^2 p_{O_2}^2, \quad (55)$$

where the binding constant  $K$  is the product of a temperature-dependent factor and a temperature-independent constant

$$K = C \exp(-U/kT). \quad (56)$$

Eqn (53) can be written in the same form as eqn (55) by dividing through by the factor  $(1 + \exp(-U_q^*/kT))$ , with the result

$$Z_{\text{MWC/Perutz}} = 1 + 2 \left( \frac{K_{\text{deoxy}} + \exp(-U_q^*/kT) K_{\text{oxy}}}{1 + \exp(-U_q^*/kT)} \right) p_{O_2} + \left( \frac{K_{\text{deoxy}}^2 + \exp(-U_q^*/kT) K_{\text{oxy}}^2}{1 + \exp(-U_q^*/kT)} \right) p_{O_2}^2. \quad (57)$$

The fraction of hemes oxygenated is calculated from the partition function of eqn (53), (55) or (57) using the relation

$$Y_{O_2} = \frac{1}{2} \left( \frac{\partial \ln Z}{\partial \ln p_{O_2}} \right). \quad (58)$$

Notice that at a single temperature, the  $p_{O_2}$  dependence of oxygenation of a dimer is of the same form for the two models described by eqns (55) and (57). However, the variation with temperature is different in the two cases. Thus by observing the temperature dependence of oxygenation one should, in principle, be able to determine which model best describes co-operativity in the dimer. For mollusc myoglobin, the best fit using the four parameters of the set of simultaneous equations (53), (54) and

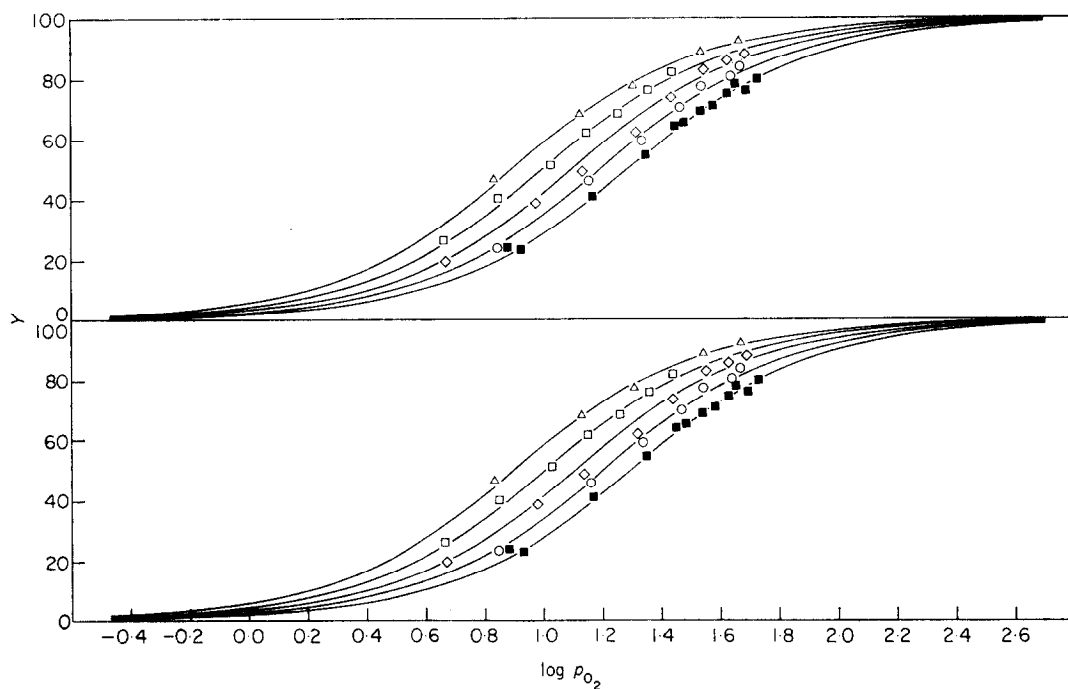


FIG. 14. Oxygenation data of Terwilliger & Read (1971) for the myoglobin of the mollusc *Buccinum undatum*, and comparison with theoretical equilibrium curves. Data are taken at pH 7.4, with  $7.5 \times 10^{-5}$  M-myoglobin (by dimer) in 0.1 M- $\text{Na}_2\text{PO}_4/\text{NaCl}$  buffer. The temperatures shown are identified by the following symbols: ( $\Delta$ ) 10°C, ( $\square$ ) 15°C, ( $\diamond$ ) 20°C, ( $\circ$ ) 25°C, and ( $\blacksquare$ ) 30°C. (a) Theoretical equilibrium curves shown for the parameter values  $C = 1.89 \times 10^{-7}$  mm Hg $^{-1}$ ,  $U_i^* = 0.038$  eV,  $U_{\text{deoxy}} = 0.028$  eV, and  $U_{\text{oxy}} = -0.146$  eV. (b) Theoretical equilibrium curves using the parameter values  $C = 1.42 \times 10$  mm Hg $^{-1}$ ,  $U_{\text{H}} = 0.011$  eV, and  $U = -0.322$  eV.

(58) is shown in Figure 14(a). The best fit using the three parameters of eqns (55), (56) and (58) is shown in Figure 14(b). The two sets of theoretical curves are almost identical for the temperatures shown. This is because within this limited range of temperatures, eqn (57) can be approximated by the expression

$$Z_{\text{MWC/Perutz}} \cong 1 + 2 \exp(-U_q^*/kT) \left( \frac{K_{\text{oxy}}}{1.1} \right) p_{\text{O}_2} + \exp(-U_q^*/kT) \left( \frac{K_{\text{oxy}}}{1.1} \right)^2 p_{\text{O}_2}^2 \quad (59)$$

since  $K_{\text{deoxy}} \ll K_{\text{oxy}}$  (i.e.  $U_{\text{deoxy}} \gg U_{\text{oxy}}$ ) and  $\exp(-U_q^*/kT) < 1$ . Eqn (59) has the same temperature dependence as eqn (55). Thus in order to determine which co-operative model describes this system best, data over a wider range of temperature are required.

## 8. Concluding Discussion

In the preceding sections, equations developed for a general model of co-operativity have been utilized to describe a wide variety of ligand binding data.

In section 5 we fit data for oxygenation of HbA, data for oxygenation of the  $\beta$  chains of HbA, and data for P<sub>2</sub>Glyc binding to HbA. In contrast to the very recent work of Szabo & Karplus (1972) which describes only the dependence of  $p_{1/2}$  on P<sub>2</sub>Glyc concentration, we have fit the *full oxygenation curves* and thus our approach describes not only the P<sub>2</sub>Glyc dependence of  $p_{1/2}$  but also the P<sub>2</sub>Glyc dependence of the Hill coefficient,  $n_{\text{H}}$ , and the phenomenon of biphasic oxygenation.

Whereas Tyuma *et al.* (1971) use an Adair approach that requires a different set of four Adair parameters to describe oxygenation data at *each* P<sub>2</sub>Glyc concentration, our approach describes oxygenation at an arbitrarily large number of P<sub>2</sub>Glyc concentrations using a *total* of only five to seven parameters (depending on the details in which we are interested). (For example, according to the Tyuma approach, 20 parameters would be varied to fit five curves, while with our approach the same five curves can be fit with just five parameters if desired.) Unlike the parameters that appear in the Adair approach, the parameters in our model are chosen to represent microscopic features of the protein molecule. This allows one to predict the behavior of hemoglobin under a wide range of conditions from data taken in a limited range of conditions. The agreement we found in this fashion is clearly one reason to prefer our approach over any approach using Adair parameters, for which this test is in principle impossible.

We conclude (cf. section 5) that inhibition by P<sub>2</sub>Glyc is due primarily to its preferential binding to the deoxy quaternary conformation (a statement few would disagree with today); we *also* conclude that P<sub>2</sub>Glyc further inhibits oxygenation by strengthening molecular constraints. Moreover, we conclude that differences between the  $\alpha$  and  $\beta$  chains do not have a significant role in P<sub>2</sub>Glyc binding or inhibition (contrary to the common view).

The result, predicted by our model, that the change from the deoxy to the oxy quaternary conformation occurs at about the third oxygenation is borne out by the experimental observations of Gibson & Parkhurst (1968), Hopfield *et al.* (1972), and Heustis & Raftery (1972a).

In addition, our model allows one to calculate the P<sub>2</sub>Glyc dependence of the Adair parameters and also the P<sub>2</sub>Glyc dependence of the apparent free energy of interaction,  $\Delta F$ .

In section 5 the model explained in some detail the relation between the phenomenon of biphasic oxygenation and the dependence of the Hill coefficient,  $n_{\text{H}}$ , on P<sub>2</sub>Glyc concentration, pH, and ionic strength. This effect of pH on  $n_{\text{H}}$  is a result of

the effect of  $H^+$  on  $P_2$ Glyc binding; the separate influence of pH on  $n_H$ , due to the stabilizing effect of  $H^+$  on the deoxy tertiary conformation of each subunit, has recently been discussed by Szabo & Karplus (1972).

We considered in section 6 the effect of changes in the level of subunit aggregation on the oxygen binding equilibrium for HbA and for lamprey hemoglobin. By fitting oxygenation data for HbA at a number of concentrations, we find that the great increase in dissociation of the tetramer on oxygenation is due primarily to the high oxygen affinity of the dimer, rather than to the relatively small difference in stability between the oxy and the deoxy quaternary conformations of the tetramer. For lamprey hemoglobin we find that in addition to monomeric and dimeric molecules, tetrameric hemoglobin is present. However, since the tetramer is present only in small quantities, we are not able to tell whether it is co-operative or not.

Finally, we showed the utility of temperature-dependent data in distinguishing between different co-operative mechanisms for certain systems. However, we find that in order to apply this method, very accurate oxygenation data are required over a rather wide range of temperature.

In summary, then, the fact that the general model proposed (and solved explicitly in the Appendix) can, by varying only a few microscopic parameters, fit a wide range of different types of experimental data gives one some confidence in the values of the parameters and lends weight to the results obtained.

## APPENDIX

### Calculation of the Partition Function for a General System

In the text it was made clear that from the partition function  $Z$  one can calculate experimentally measurable quantities such as  $Y_{O_2}$ , and  $\bar{Y}_{P_2Glyc}$ . Although most of the applications in the text were to the specific system of adult human hemoglobin, it is important to emphasize that our calculational method is applicable to any system composed of subunits and displaying co-operativity. Accordingly, we derive here the general expression for the partition function of an arbitrary co-operative system.

#### (a) State variables

In order to calculate the partition function of eqn (3), we need to know the energies of all the microscopically distinguishable states of the system. In order to write an expression for these energies, we need a notation for specifying the states of the system. For example, for the case of HbA tetramer in the absence of effectors, the  $2^4 \times 2^4 \times 2 = 2^9 = 512$  possible states, were represented by the notation

$$\begin{aligned} \text{state} &= (\mathcal{O}_1, \mathcal{O}_2, \mathcal{O}_3, \mathcal{O}_4; t_1, t_2, t_3, t_4; q) \\ &= (\{\mathcal{O}_i\}, \{t_i\}, q), \quad (i = 1, \dots, N) \end{aligned}$$

where  $\mathcal{O}_i = 0,1$  when the substrate binding site on the  $i$ th subunit is empty or occupied, respectively,  $t_i = 1,2$  when the  $i$ th subunit is in the deoxy or oxy tertiary conformation, and  $q = 1,2$  when the tetramer is in the deoxy or oxy quaternary conformation.

Here we generalize this notation to include an arbitrary protein molecule composed of  $N$  subunits. Each subunit can have  $\bar{M}$  ligand binding sites; some of these sites are for substrate and some are for effectors. In addition, there may be  $\bar{M}$  additional effector binding sites which are not associated with individual subunits, but rather are associated with the molecule as a whole. Thus we allow for a total of  $\bar{M}N + \bar{M}$  binding sites.

(b) *Notation for binding*

Let the state variables describing the occupancy of these  $\bar{M}N + \bar{M}$  binding sites be denoted by the symbols  $\bar{\theta}_{ji}$  and  $\bar{\theta}_k$ , where  $\bar{\theta}_{ji} = 0, 1$  when the  $j$ th binding site on the  $i$ th subunit is empty or occupied, respectively ( $i = 1, 2, \dots, N$  and  $j = 1, \dots, \bar{M}$ ) and  $\bar{\theta}_k = 0, 1$  when the  $k$ th effector binding site of the molecule is empty or occupied ( $k = 1, \dots, \bar{M}$ ). Clearly the occupancy of all  $\bar{M}N + \bar{M}$  binding sites is specified by a knowledge of all the  $\bar{M}N + \bar{M}$  state variables  $\bar{\theta}_{ji}$  and  $\bar{\theta}_k$ .

(c) *Notation for tertiary structure*

We use the notation  $t_i$  to denote the state variable describing the tertiary conformation of the  $i$ th subunit. In general,  $t_i = 1, 2, \dots, \bar{m}$ , corresponding to the fact that each subunit can have  $\bar{m}$  possible tertiary conformations. The set of  $N$  variables  $\{t_1, \dots, t_N\}$  completely specifies the tertiary conformations of all  $N$  subunits of the protein molecule.

(d) *Notation for quaternary structure*

We use the notation  $q$  to denote the state variable describing the quaternary conformation of the molecule. We allow for an arbitrary number  $\bar{m}$  of possible quaternary conformations and these are represented by  $q = 1, 2, \dots, \bar{m}$ . For each of the  $\bar{m}$  quaternary conformations,  $N$  specifies the number of subunits in the oligomer.

(e) *The partition function for the general system*

The partition function may be directly expressed in terms of the state variables defined above. The partition function involves a summation over all possible microstates of the system, and in general has a total of  $\sum_{q=1}^{\bar{m}} 2^{\bar{M}N + \bar{M}} \bar{m}^N$  terms. It is given by the multiple sum

$$Z = \sum_{q=1}^{\bar{m}} \left\{ \sum_{t_1=1}^{\bar{m}} \dots \sum_{t_N=1}^{\bar{m}} \right\} \left\{ \sum_{\bar{\theta}_{11}=0}^1 \dots \sum_{\bar{\theta}_{\bar{M}N}=0}^1 \right\} \left\{ \sum_{\bar{\theta}_1=0}^1 \dots \sum_{\bar{\theta}_{\bar{M}}=0}^1 \right\} \\ \times \exp[-\mathcal{E}(\bar{\theta}_{11} \dots \bar{\theta}_{\bar{M}N}; \bar{\theta}_1 \dots \bar{\theta}_{\bar{M}}; t_1 \dots t_N; q)/kT]. \quad (\text{A1})$$

Equation (A1) may be written in the following convenient abbreviated notation

$$Z = \sum_q \sum_{\{t\}} \sum_{\{\bar{\theta}\}} \sum_{\{\bar{\theta}\}} \exp[-\mathcal{E}(\{\bar{\theta}\}; \{\bar{\theta}\}; \{t\}; q)/kT]. \quad (\text{A2})$$

In generalization of eqn (3),

$$\mathcal{E}(\{\bar{\theta}\}; \{\bar{\theta}\}; \{t\}; q) = E(\{\bar{\theta}\}, \{\bar{\theta}\}, \{t\}, q) - N\mu_p - \sum_{i=1}^N \sum_{j=1}^{\bar{M}} \bar{\theta}_{ji} \bar{\mu}_{ji} - \sum_{k=1}^{\bar{M}} \bar{\theta}_k \bar{\mu}_k. \quad (\text{A3})$$

Here  $\mu_p$  is the chemical potential of unliganded, monomeric protein,  $\bar{\mu}_{j_i}$  is the chemical potential of the ligand that binds to the  $j$ th site of the  $i$ th subunit, and  $\bar{\mu}_k$  is the chemical potential of the ligand which binds to the  $k$ th effector site of the *molecule*. Note that since the subunits are assumed equivalent, the same type of ligand binds to the  $j$ th site on all subunits and therefore  $\bar{\mu}_{j_1} = \bar{\mu}_{j_2} = \dots = \bar{\mu}_{j_N} = \bar{\mu}_j$ . (Also, two different sites,  $j$  and  $l$ , on a subunit may bind the same type of ligand (e.g. two different acid groups both bind hydrogen ions), in which case  $\bar{\mu}_j = \bar{\mu}_l$ .)

We can express the energy,  $E$ , of a particular *molecular* state as the sum

$$\begin{aligned} E(\bar{\mathcal{O}}_{11}, \dots, \bar{\mathcal{O}}_{MN}; \bar{\mathcal{O}}_1, \dots, \bar{\mathcal{O}}_{\bar{M}}; t_1, \dots, t_N; q) \\ = E_C(t_1, \dots, t_N; q) \\ + E_L(\bar{\mathcal{O}}_{11}, \dots, \bar{\mathcal{O}}_{MN}; \bar{\mathcal{O}}_1, \dots, \bar{\mathcal{O}}_{\bar{M}}|t_1, \dots, t_N; q), \end{aligned} \tag{A4}$$

where  $E_C(t_1, \dots, t_N; q)$  represents the conformational energy of a molecule in the  $\{t_1, \dots, t_N; q\}$  conformational state in the absence of ligand binding, and  $E_L(\bar{\mathcal{O}}_{11}, \dots, \bar{\mathcal{O}}_{MN}; \bar{\mathcal{O}}_1, \dots, \bar{\mathcal{O}}_{\bar{M}}|t_1, \dots, t_N; q)$  represents the added energy due to the ligand binding  $[\bar{\mathcal{O}}_{11}, \dots, \bar{\mathcal{O}}_{MN}; \bar{\mathcal{O}}_1, \dots, \bar{\mathcal{O}}_{\bar{M}}]$ , to a molecule which is in the conformational state  $[t_1, \dots, t_N; q]$ .

Now  $E_L$  may be divided up as follows:

$$\begin{aligned} E_L(\bar{\mathcal{O}}_{11}, \dots, \bar{\mathcal{O}}_{MN}; \bar{\mathcal{O}}_1, \dots, \bar{\mathcal{O}}_{\bar{M}}) = \sum_{i=1}^N E_T(\bar{\mathcal{O}}_{1i}, \dots, \bar{\mathcal{O}}_{Mi}|t_i) \\ + E_Q(\bar{\mathcal{O}}_1, \dots, \bar{\mathcal{O}}_{\bar{M}}|q), \end{aligned} \tag{A5}$$

where  $E_T(\bar{\mathcal{O}}_{1i}, \dots, \bar{\mathcal{O}}_{Mi}|t_i)$  is the energy due to the ligand binding  $[\bar{\mathcal{O}}_{1i}, \dots, \bar{\mathcal{O}}_{Mi}]$  to the  $i$ th subunit when it is in the  $t_i$  tertiary conformation. Similarly,  $E_Q(\bar{\mathcal{O}}_1, \dots, \bar{\mathcal{O}}_{\bar{M}}|q)$  is the energy due to the ligand binding  $[\bar{\mathcal{O}}_1, \dots, \bar{\mathcal{O}}_{\bar{M}}]$  to the molecule when it is in the  $q$  quaternary conformation. Substituting eqns (A2) to (A5) into eqn (A1) we have

$$\begin{aligned} Z = \sum_{q=1}^{\bar{m}} \sum_{t_1=1}^{\bar{m}} \dots \sum_{t_N=1}^{\bar{m}} \exp[(-E_C(t_1, \dots, t_N; q)/kT) + (N\mu_p/kT)] \\ \times \sum_{\bar{o}_{11}=0}^1 \dots \sum_{\bar{o}_{MN}=0}^1 \prod_{i=1}^N \exp[(-E_T(\bar{\mathcal{O}}_{1i}, \dots, \bar{\mathcal{O}}_{Mi}|t_i)/kT) + \sum_{k=1}^{\bar{M}} \bar{\mathcal{O}}_{ki}\mu_{ki}/kT] \\ \times \sum_{\bar{o}_1=0}^1 \dots \sum_{\bar{o}_{\bar{M}}=0}^1 \exp[(-E_Q(\bar{\mathcal{O}}_1, \dots, \bar{\mathcal{O}}_{\bar{M}}|q)/kT) + \sum_{k=1}^{\bar{M}} \bar{\mathcal{O}}_k\mu_k/kT]. \end{aligned} \tag{A6}$$

It is convenient to define two functions, which represent partial sums contributing to eqn (A6). By analogy with eqns (A1) to (A3), the "partition function" for ligand binding to a *single subunit in the  $t_i$  conformation* is defined as the multiple sum

$$Z_T(t_i) = \sum_{\bar{o}_{1i}=0}^1 \dots \sum_{\bar{o}_{Mi}=0}^1 \bar{\rho}(\bar{\mathcal{O}}_{1i}, \dots, \bar{\mathcal{O}}_{Mi}|t_i), \tag{A7}$$

where

$$\bar{\rho}(\bar{\mathcal{O}}_{1i}, \dots, \bar{\mathcal{O}}_{Mi}|t_i) = \exp(-[E_T(\bar{\mathcal{O}}_{1i}, \dots, \bar{\mathcal{O}}_{Mi}|t_i) + \sum_{k=1}^{\bar{M}} \bar{\mathcal{O}}_{ki}\mu_{ki}]/kT) \tag{A8}$$

is the unnormalized probability that a protomer in the  $t_i$  conformational state will be in the  $\{\bar{\mathcal{O}}_{1i}, \dots, \bar{\mathcal{O}}_{Mi}\}$  ligand binding state. Similarly the "partition function" for ligand binding to a *molecule in the  $q$  conformation* is defined as

$$Z_Q(q) = \sum_{\tilde{\sigma}_1=0}^1 \cdots \sum_{\tilde{\sigma}_M=0}^1 \beta(\tilde{\sigma}_1, \dots, \tilde{\sigma}_M|q), \quad (\text{A9})$$

where

$$\beta(\tilde{\sigma}_1, \dots, \tilde{\sigma}_M|q) = \exp(-[E_Q(\tilde{\sigma}_1, \dots, \tilde{\sigma}_M|q) + \sum_{k=1}^M \tilde{\sigma}_k \mu_k]/kT). \quad (\text{A10})$$

Combining eqns (A6) to (A10), we can rewrite the grand partition function as

$$Z = \sum_{q=1}^{\bar{m}} \sum_{t_1=1}^{\bar{m}} \cdots \sum_{t_N=1}^{\bar{m}} \exp[(-E_Q(t_1, \dots, t_N; q)/kT) + N\mu_p/kT] \left[ \prod_{i=1}^N Z_T(t_i) \right] Z_Q(q). \quad (\text{A11})$$

The conformational energy  $E_C$  consists of a number of different components:

$$E_C(t_1, \dots, t_N; q) = \sum_{j=1}^N E_t(t_j) + E_q(q) + \sum_{j=1}^N E_{tq}(t_j, q) + \sum_{j=1}^N E_{tt}(t_j, t_{j+1}|q), \quad (\text{A12})$$

where  $E_t(t_j)$  is the energy of the  $t_j$  tertiary conformation in the absence of constraints,  $E_q(q)$  is the energy of the  $q$  quaternary conformation in the absence of constraints,  $E_{tq}(t_j, q)$  is the energy of the  $q$ - $t$  interaction between the  $q$  quaternary conformation of the molecule and the  $t_j$  tertiary conformation of the  $j$ th subunit, and  $E_{tt}(t_j, t_{j+1}|q)$  is the energy of the  $t$ - $t$  interaction between a pair of neighboring subunits, with tertiary conformations  $t_j$  and  $t_{j+1}$ , when the molecule is in the  $q$  quaternary conformation. (Note that, for a ring of  $N$  protomers, the  $(N+1)$ th protomer is the same as the first, then  $E_{tt}(t_N, t_{N+1}|q)$  represents the interaction between the  $N$ th and the first protomers.)

Substituting eqn (A12) into eqn (A11) we get

$$Z = \sum_{q=1}^{\bar{m}} Z_Q(q) \exp(-E_q(q)/kT) \exp(N\mu_p/kT) \sum_{t_1=1}^{\bar{m}} \cdots \sum_{t_N=1}^{\bar{m}} \times \prod_{j=1}^N Z_T(t_j) \exp(-[E_t(t_j) + E_{tq}(t_j, q) + E_{tt}(t_j, t_{j+1}|q)]/kT). \quad (\text{A13})$$

It is convenient to rewrite this partition function in the symmetrized form

$$Z = \sum_{q=1}^{\bar{m}} Z_Q(q) \exp(-E_q(q)/kT) \exp(N\mu_p/kT) z(q), \quad (\text{A14})$$

where

$$z(q) \equiv \sum_{t_1=1}^{\bar{m}} \cdots \sum_{t_N=1}^{\bar{m}} \prod_{j=1}^N A_q(t_j, t_{j+1}) \quad (\text{A15})$$

and the terms of the  $\bar{m} \times \bar{m}$  symmetric "transfer matrix"  $A_q$ , are

$$\begin{aligned} A_q(t_j, t_{j+1}) &= A_q(t_{j+1}, t_j) \\ &= [Z_T(t_j) Z_T(t_{j+1})]^{1/2} \exp[-\{1/2[E_t(t_j) + E_t(t_{j+1})] \\ &\quad + 1/2[E_{tq}(t_j, q) + E_{tq}(t_{j+1}, q)] \\ &\quad + E_{tt}(t_j, t_{j+1}, q)\}/kT\}]. \end{aligned} \quad (\text{A16})$$

This use of the symmetric  $\bar{m} \times \bar{m}$  transfer matrix to evaluate  $Z$  is a generalization of the  $2 \times 2$  transfer matrix commonly used for Ising models (see, e.g., Stanley, 1971) and applied by Thompson (1968) to the Koshland model. Using matrix algebra we obtain

$$\begin{aligned} z(q) &= \sum_{t_1=1}^{\bar{m}} \dots \sum_{t_{N-1}=1}^{\bar{m}} A_q(t_1, t_2) A_q(t_2, t_3) \dots A_q(t_{N-1}, t_N) A_q(t_N, t_1) \\ &= \sum_{t_1=1}^{\bar{m}} \dots \sum_{t_{N-1}=1}^{\bar{m}} A_q(t_1, t_2) A_q(t_2, t_3) \dots A_q(t_{N-2}, t_{N-1}) A_q^2(t_{N-1}, t_1) \\ &= \sum_{t_1=1}^{\bar{m}} A_q^N(t_1, t_1) = \text{trace} (A_q^N) \\ &= \sum_{j=1}^{\bar{m}} [\chi_j(q)]^N, \end{aligned} \tag{A17}$$

where  $\chi_j(q)$  is the  $j$ th eigenvalue of the transfer matrix  $A_q$ . The  $\bar{m}$  eigenvalues  $\chi_j(q)$  ( $j = 1, 2, \dots, \bar{m}$ ) are the roots of the  $\bar{m}$ th order equation

$$|A_q - \chi(q) I| = 0. \tag{A18}$$

Combining eqns (A14) to (A16) we have for the partition function

$$Z = \sum_{q=1}^{\bar{m}} Z_Q(q) \exp(-E_q(q)/kT) \exp(N\mu_p/kT) \sum_{j=1}^{\bar{m}} [\chi_j(q)]^N. \tag{A19}$$

(f) *Partition function for a useful special case*

Eqn (A19) applies for any values of  $\bar{m}$ ,  $\bar{m}$ ,  $\bar{M}$  and  $\bar{M}$ . However, the single case of  $\bar{m} = 2$ ,  $\bar{m} = 2$ ,  $\bar{M} = 1$ , and  $\bar{M} = 0$ , for a non-dissociating protein molecule of  $N$  subunits, is the most readily solved and is sufficient to display both the t-q and the t-t modes of *homotropic* allosteric coupling. It is also directly applicable to the oxygen equilibrium of hemoglobin. For this case there are two quaternary conformations, represented by  $q = 1$  and  $q = 2$ , reversibly accessible to the molecule ( $\bar{m} = 2$ ); two tertiary conformations, represented by  $t = 1$  and  $t = 2$ , are reversibly accessible to each subunit ( $\bar{m} = 2$ ); and there is one substrate site on each subunit and no effectors are present ( $\bar{M} = 1$  and  $\bar{M} = 0$ ).

In this case, the energies defined in eqns (A5) and (A12) may be expressed, with a convenient choice of the zero of energy, as

$$E_T(\mathcal{O}_{sj}|t_j) = \mathcal{O}_{sj}[U_o + (-1)^{t_j} U_{ot}] \tag{A20}$$

(where the subscript  $s$  denotes the substrate binding site of a particular subunit). We have

$$\begin{aligned} E_Q &= 0 \\ E_t(t_j) &= (t_j - 1) U_t \\ E_q(q) &= (q - 1) U_q \\ E_{tt}(t_j, t_j + 1|q) &= - (-1)^{t_j} (-1)^{t_j+1} U_{tt}(q) \\ E_{tq}(t_j, q) &= - (-1)^{t_j} (-1)^q U_{qt}, \end{aligned}$$

where the choice of parameters is explained in section 3 of the main paper.

The functional dependence of  $Z$  on the various parameters may be determined by the method outlined above. From eqn (A16) the elements of the  $2 \times 2$  transfer matrix for the case  $\bar{m} = 2$  and  $\tilde{m} = 2$  are

$$\mathbf{A}_q = \begin{bmatrix} \exp(U_{tt}(q)/kT)\phi(1|q) & \exp(-U_{tt}(q)/kT)[\phi(1|q)\phi(2|q)]^{1/2} \\ \exp(-U_{tt}(q)/kT)[\phi(1|q)\phi(2|q)]^{1/2} & \exp(U_{tt}(q)/kT)\phi(2|q) \end{bmatrix}. \quad (\text{A21})$$

The equation for the eigenvalues is

$$0 = |\mathbf{A}_q - \chi(q)\mathbf{I}| = [\exp(U_{tt}(q)/kT)\phi(1|q) - \chi(q)][\exp(U_{tt}(q)/kT)\phi(2|q) - \chi(q)] - \exp(-2U_{tt}(q)/kT)\phi(1|q)\phi(2|q), \quad (\text{A22})$$

with solutions

$$\begin{aligned} \chi_{1,2}(q) &= \exp(U_{tt}(q)/kT) [\phi(1|q) + \phi(2|q)]/2 \\ &\pm \{\exp(2U_{tt}(q)/kT) ([\phi(1|q) - \phi(2|q)]/2)^2 \\ &+ \exp(-2U_{tt}(q)/kT)\phi(1|q)\phi(2|q)\}^{1/2}, \end{aligned} \quad (\text{A23})$$

where

$$\phi(t|q) = \exp(-U_t/kT) \exp(U_{qt}(-1)^{t+q}/kT) Z_T(t). \quad (\text{A24})$$

From eqn (A19) we have for the partition function

$$Z = Z_Q(1) \{[\chi_1(1)]^N + [\chi_2(1)]^N\} + Z_Q(2) \exp(-U_q/kT) \{[\chi_1(2)]^N + [\chi_2(2)]^N\}. \quad (\text{A25})$$

(Here the zero of energy has been shifted by the constant  $N\mu_p$ .)

From eqns (A7) to (A10) for the case  $\bar{M} = 1$  and  $\tilde{M} = 0$ ,

$$Z_T(t) = \exp([\mu_s - (U_o + (-1)^t U_{ot})/kT] + 1) \quad (\text{A26})$$

and

$$Z_Q(q) = 1, \quad (\text{A27})$$

where  $\mu_s$  is the chemical potential of the substrate.

The first author (J. H.) is sincerely grateful to Professor Robert J. Silbey, of the Massachusetts Institute of Technology (M.I.T.) Chemistry Department, for his generous moral and financial support of this work. Professor Franklin Bunn, of Harvard Medical School and Children's Hospital, was very kind to go out of his way to take a set of biphasic oxygenation data for us. In addition to enlightening discussions with Professor Bunn, we are grateful for the comments and suggestions of Professors Ruth and Reinhold Benesch of Columbia University, Professor Jean-Pierre Changeux of the Pasteur Institute, and Professor John Hopfield of Princeton University. We are much obliged to Mr Arnold Reinhold for his painstaking and astute guidance in the programming aspects of this endeavor and for the loan of an excellent maximizing routine. We also thank Rama Daga Bansil for the benefits of our many discussions on this subject.

Some of this work is included in a Ph.D. thesis submitted to M.I.T. by one of us (J.H.). The work was supported by the Research Corporation, by the National Science Foundation through the M.I.T. Center for Materials Science and Engineering, by the National Heart and Lung Institute (grant HL14322-02) and a National Institutes of Health Biomedical Sciences support grant (NIH-5-S05-RR07047-08) to M.I.T.

## REFERENCES

- Adair, G. S. (1925a). *Proc. Roy. Soc., London (Ser. A)*, **109**, 292-300.
- Adair, G. S. (1925b). *J. Biol. Chem.* **63**, 529-545.
- Arnone, A. (1972). *Nature (London)*, **237**, 146-149.
- Bauer, C. (1970). *Resp. Physiol.* **10**, 10-19.
- Benesch, R. E., Benesch, R. & Yu, C. Y. (1969). *Biochemistry*, **8**, 2567-2571.
- Briehl, R. W. (1963). *J. Biol. Chem.* **238**, 2361-2366.
- Bunn, H. F. & Briehl, R. W. (1970). *J. Clin. Invest.* **49**, 1088-1095.
- Caldwell, P. R. B., Nagel, R. L. & Jaffe, E. R. (1971). *Biochem. Biophys. Res. Commun.* **44**, 1504-1509.
- Davidson, N. (1962). *Statistical Mechanics*, McGraw-Hill, New York.
- Edelstein, S. J., Rehmar, M. J., Olson, J. S. & Gibson, Q. H. (1970). *J. Biol. Chem.* **245**, 4372-4381.
- Gibson, Q. H. & Parkhurst, L. J. (1968). *J. Biol. Chem.* **243**, 5521-5524.
- Herzfeld, J. & Stanley, H. E. (1972a). *Biochem. Biophys. Res. Commun.* **48**, 307-313.
- Herzfeld, J. & Stanley, H. E. (1972b). *Biomedical Physics and Biomaterials Science, Proceedings of the 1971 M.I.T. Summer School* (H. E. Stanley, ed.), chap. 4, M.I.T. Press, Cambridge, Mass.
- Heustis, W. H. & Raftery, M. A. (1972a). *Biochem. Biophys. Res. Commun.* **49**, 428-433.
- Heustis, W. H. & Raftery, M. A. (1972b). *Biochem. Biophys. Res. Commun.* **49**, 1358-1365.
- Hopfield, J., Ogawa, S. & Shulman, R. G. (1972). *Biochem. Biophys. Res. Commun.* **49**, 1480-1484.
- Kellett, G. L. (1971). *J. Mol. Biol.* **59**, 401-424.
- Kellett, G. L. & Gutfreund, H. (1970). *Nature (London)*, **227**, 921-926.
- Koshland, D. E., Nemethy, G. & Filmer, D. (1966). *Biochemistry*, **5**, 365-385.
- Monod, J., Wyman, J. & Changeux, J.-P. (1965). *J. Mol. Biol.* **12**, 88-118.
- Ogata, R. T. & McConnell, H. M. (1972a). *Proc. Nat. Acad. Sci., U.S.A.* **69**, 335-339.
- Ogata, R. T. & McConnell, H. M. (1972b). *Biochemistry*, **11**, 4792-4799.
- Pauling, L. (1935). *Proc. Nat. Acad. Sci., U.S.A.* **21**, 186-191.
- Perutz, M. F. (1970a). *Nature (London)*, **228**, 726-734.
- Perutz, M. F. (1970b). *Nature (London)*, **228**, 734-739.
- Roughton, F. J. W. & Lyster, R. L. J. (1965). *Havardadets Skrifter*, **48**, 185-198.
- Salhany, J. M., Mathers, D. H. & Eliot, R. S. (1972). *J. Biol. Chem.* **247**, 6985-6990.
- Stanley, H. E. (1971). *Introduction to Phase Transitions and Critical Phenomena*, Oxford University Press, London.
- Szabo, A. & Karplus, M. (1972). *J. Mol. Biol.* **72**, 163-197.
- Terwilliger, R. C. & Read, K. R. H. (1971). *Int. J. Biochem.* **2**, 253-261.
- Thomas, J. O. & Edelstein, S. J. (1972). *J. Biol. Chem.* **247**, 7870-7874.
- Thompson, C. J. (1968). *Biopolymers*, **6**, 1101-1118.
- Tomita, S. & Riggs, A. (1971). *J. Biol. Chem.* **246**, 547-554.
- Tyuma, I., Shimizu, K. & Imai, K. (1971). *Biochem. Biophys. Res. Commun.* **43**, 423-428.
- Whitehead, E. (1970). *Prog. Biophys. & Mol. Biol.* **21**, 323-397.
- Wyman, J. (1965). *J. Mol. Biol.* **11**, 631-644.
- Wyman, J. (1967). *J. Amer. Chem. Soc.* **89**, 2202-2218.
- Wyman, J. (1968). *Quant. Rev. Biophys.* **1**, 35-80.

*Note added in proof:* It has recently been suggested to the authors that energies would be more appropriately expressed in units of kcal/mole rather than electron volts (eV). Rather than alter the manuscript in proof, we simply remind the reader that 1 eV = 23.06 kcal/mole.